Foulger Consulting

1025 Paradise Way
Palo Alto, CA 943062637, USA
Tel: 650/4932553
Cell: 650/9968886
FAX: 866/5326907
gillian@foulgerconsulting.com
http://www.foulgerconsulting.com/

October 29, 2014

WEEKLY REPORT #4 TO ALTAROCK ENERGY INC.

PROCESSING OF INDUCED EARTHQUAKES ASSOCIATED WITH THE NEWBERRY EGS INJECTION STARTING SEPTEMBER 2014

GILLIAN R. FOULGER & BRUCE R. JULIAN

Brief summary

Difficulties with transferring the full data from the ISTI system to our computers have settled down. A few channels are still missing or mis-timed, but these problems are minor and not significantly impacting the quality of the results we are able to produce.

We have completed relative relocations for the earthquakes up to 19 October with good results. The earthquakes clearly define a N 45° W striking fault, dipping at ~ 87° to the NE and activated in two depth intervals. One depth interval is the lowest ~ 250 m of the borehole and the other is ~ 200 m below the bottom of the borehole. The along-strike length of the activated fault is ~ 250 m.

During the forthcoming week we will update these results with earthquakes that occurred after 19 October, and we will also relatively locate the largest earthquakes using the high-quality arrival time measurements made for moment tensor calculations.

We derived an additional 10 moment tensors, bringing the currently available set to 34. The pattern of source types observed earlier remains constant with the addition of more results. The source types range from +Dipole to -Dipole with approximately equal numbers of earthquakes showing crack-opening and crack-closure. The T-axes, which gives an indication of the direction of σ_3, cluster sub-horizontally S±20° or so. The P- and I-axes are more scattered.

1 Task 1 – Planning, conference calls, discussion of work, correspondence, followup

We continued to maintain contact with team members. The issues associated with data completeness and formatting have subsided and the number of missing or incorrectly timed traces is now reduced. We have thus not needed to exchange many emails with ISTI, and our work has proceeded smoothly over the reporting week.

2 Task 2 – System Setup

Tailoring our system setup to the data supplied by ISTI, and tuning the relative location software parameters to the 2014 dataset is now essentially complete.

3 Task 3 – Quality control of prepicked MEQs and preparation for relocation and moment tensor calculation

We continued to derive moment tensors, prioritorising the largest earthquakes as in previous weeks. We continue to use the same procedure as described in our Weekly Report #1. We report here an additional 10 moment tensors. The entire list of earthquakes processed to date is given in

Table 1. We have provided the locations and moment tensor decomposition data of these new moment tensors to Trenton Cladouhos of AltaRock electronically, by email attachment.

Table 1: The 34 earthquakes for which moment tensors have been obtained. Locations given below are from the webpage http://fracture.lbl.gov/Newberry/locations.txt.

jday	month	day	hour	minute	sec	lat	lon	depth	magnitude
273	9	30	21	30	43.689	43.72667	-121.313	0.387	0.972
274	10	1	1	3	14.64	43.7239	-121.30957	0.714	0.987
274	10	1	8	8	58.215	43.72623	-121.31412	1.196	0.848
274	10	1	10	50	55.229	43.72275	-121.30868	1.051	0.787
274	10	1	12	3	16.881	43.72658	-121.3158	1.587	1.086
274	10	1	14	53	5.102	43.72545	-121.31355	0.613	1.381
274	10	1	15	1	55.056	43.72775	-121.31227	0.923	0.682
274	10	1	16	56	11.256	43.72232	-121.30712	1.65	0.901
274	10	1	19	5	16.377	43.72662	-121.31117	0.517	1.259
275	10	2	6	38	47.428	43.7243	-121.31328	1.153	0.951
275	10	2	6	47	52.916	43.72632	-121.31322	1.323	1.117
275	10	2	7	7	11.646	43.72488	-121.31192	0.708	1.378
275	10	2	11	1	48.042	43.72567	-121.31168	0.666	1.22
275	10	2	12	39	9.082	43.7264	-121.31438	1.332	0.852
275	10	2	18	53	48.447	43.72082	-121.31372	1.671	0.957
275	10	2	20	36	50.997	43.72377	-121.31323	1.499	0.991
276	10	3	6	6	22.727	43.72528	-121.31493	0.928	1.157
276	10	3	15	27	57.912	43.72257	-121.31562	1.054	0.919
276	10	3	18	54	54.199	43.72678	-121.31125	0.647	1.021
277	10	4	5	29	8.347	43.72578	-121.31068	0.946	0.922
277	10	4	17	32	52.716	43.72207	-121.31693	0.376	1.521
277	10	4	18	51	11.991	43.72295	-121.31227	0.496	1.97
278	10	5	2	6	17.079	43.7266	-121.31217	0.925	0.86
278	10	5	4	7	30.446	43.725	-121.31322	0.659	1.696
278	10	5	15	55	21.373	43.73483	-121.30918	0.702	0.695
278	10	5	16	7	32.904	43.7253	-121.30967	1.205	0.819
278	10	5	23	22	16.638	43.72368	-121.3116	1.055	0.931
285	10	12	10	12	29.727	43.7257	-121.3135	0.783	0.863
285	10	12	16	37	43.42	43.72515	-121.3151	0.49	1.482
285	10	12	21	10	18.995	43.72783	-121.31002	0.653	0.792
286	10	13	0	57	6.873	43.72382	-121.3175	0.242	1.197
286	10	13	4	12	29.232	43.72657	-121.30698	0.882	1.179
286	10	13	10	22	29.146	43.7302	-121.3153	0.831	0.907

287	10	14	5	46	14.161	43.71765	-121.31087	0.161	0.904

4 Task 4 –Improved locations and relative locations

4.1 Absolute locations

We updated our relocation of the earthquakes to date using **qloc**. The epicentral locations up to Oct. 26 are shown in Figure 1, and a depth vs. time plot for the same locations is shown in Figure 2.

Figure 3 shows the week-by-week development of the seismic sequence for the five weeks to date.

Figure 4 shows ISTI epicentral locations for comparison with Figure 1.

The general picture has not changed with an additional week of earthquakes. The cluster is still centered centered 100 to 200 m north of the bottom of well NWD 55-29 and is quasi-circular with a diameter of ~ 500 m.

Figure 5 and Figure 6 show the locations of the MEQs for which moment tensors were derived. These earthquakes are the largest and most accurately located earthquakes available to date. They form two clusters near the bottom of well NWD 55-29, a shallower cluster slightly to the north of the well and a deeper cluster slightly to the south. The pattern of locations of these earthquakes is similar to the relative locations (see below), providing some "ground truth" to the bimodal spatial distribution observed. Interestingly, this pattern, first reported for the moment-tensor-earthquake locations in last week's report, is now confirmed by the relative location work.

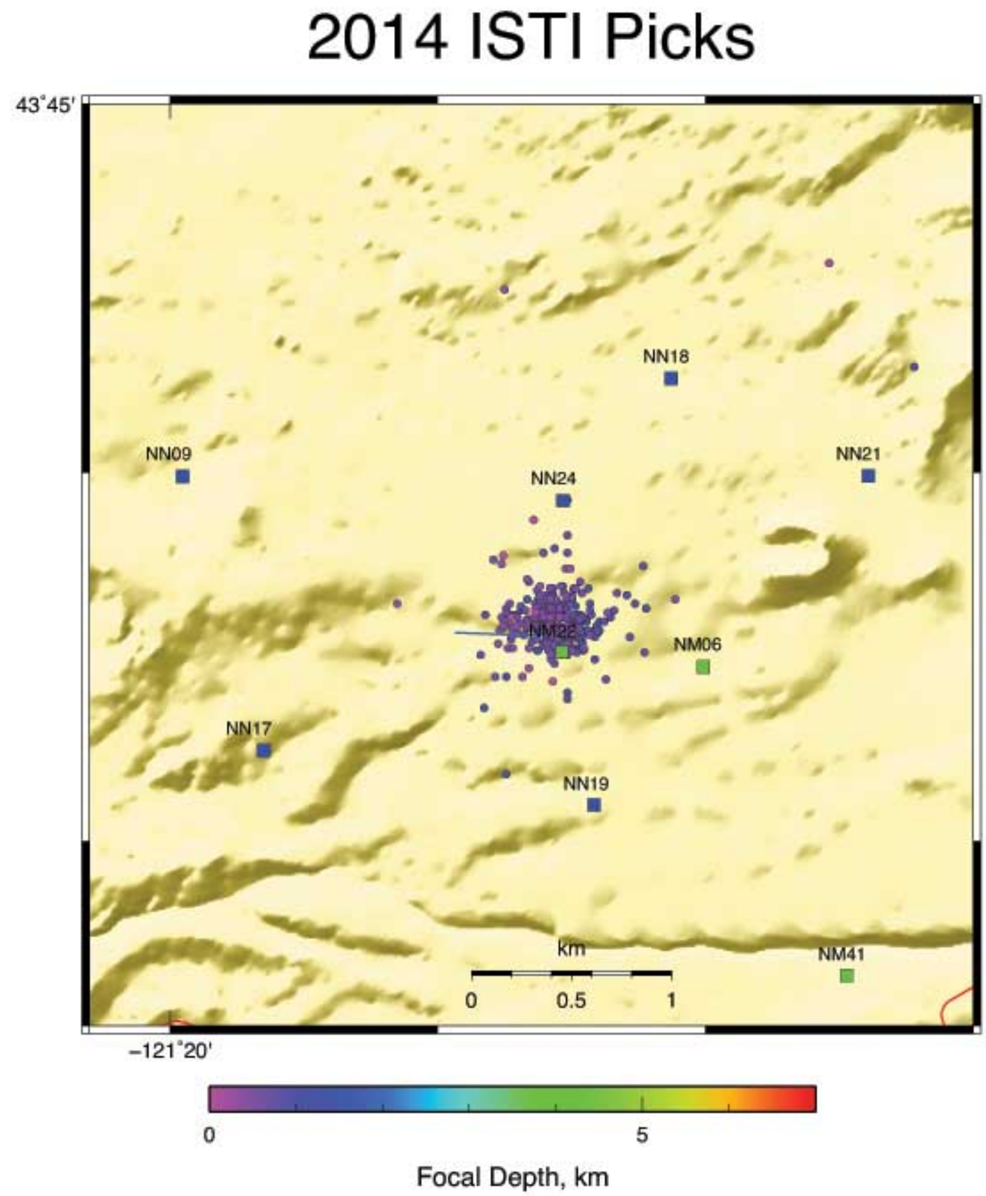

Figure 1: Estimated hypocenters of 297 microearthquakes between Sept. 26 and Oct. 26, 2014 within the NMSA network. Most events lie within a circle about 500 m in diameter and centered 100 to 200 m north of the bottom of well NWD 55-29, which is shown in blue. These locations were obtained by using the **qloc** program to invert *P*- and *S*-phase arrival times measured by personnel of the ISTI Corporation on digital seismograms from the NMSA network.

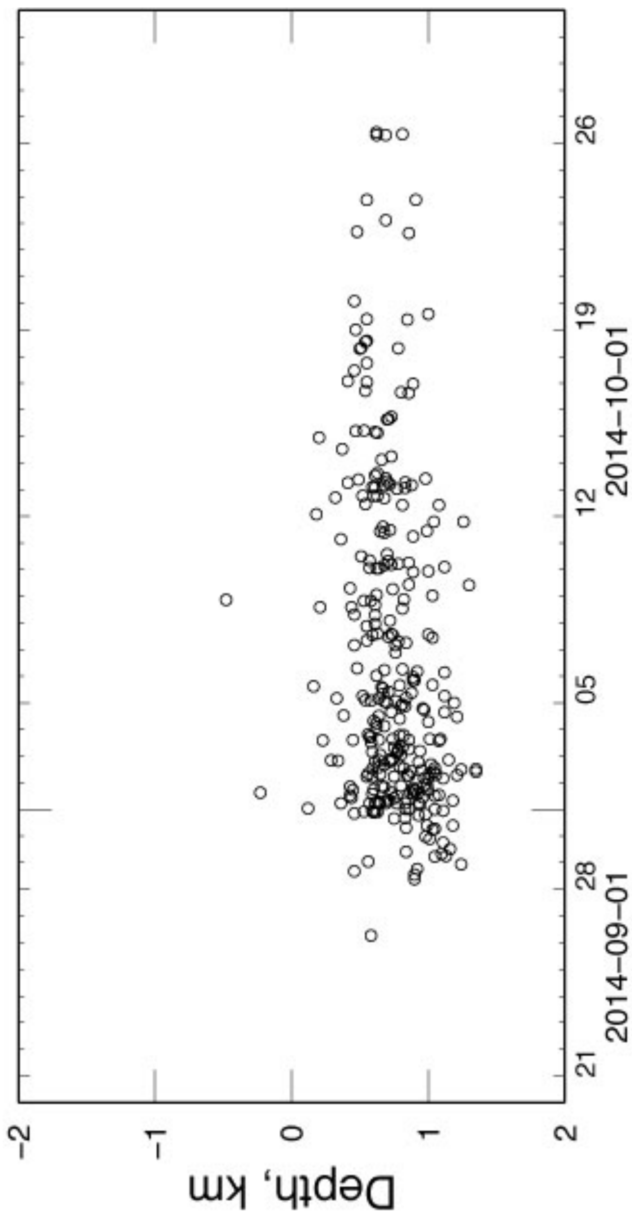

Figure 2: Estimated depths, with respect to sea level, of 297 microearthquakes within the NMSA network as a function of time. The average depth appears to be decreasing slightly with time because of a decrease in the number of deeper events. These depths were obtained by using the **qloc** program to invert *P*- and *S*-phase arrival times measured by personnel of the ISTI Corporation on digital seismograms from the NMSA network.

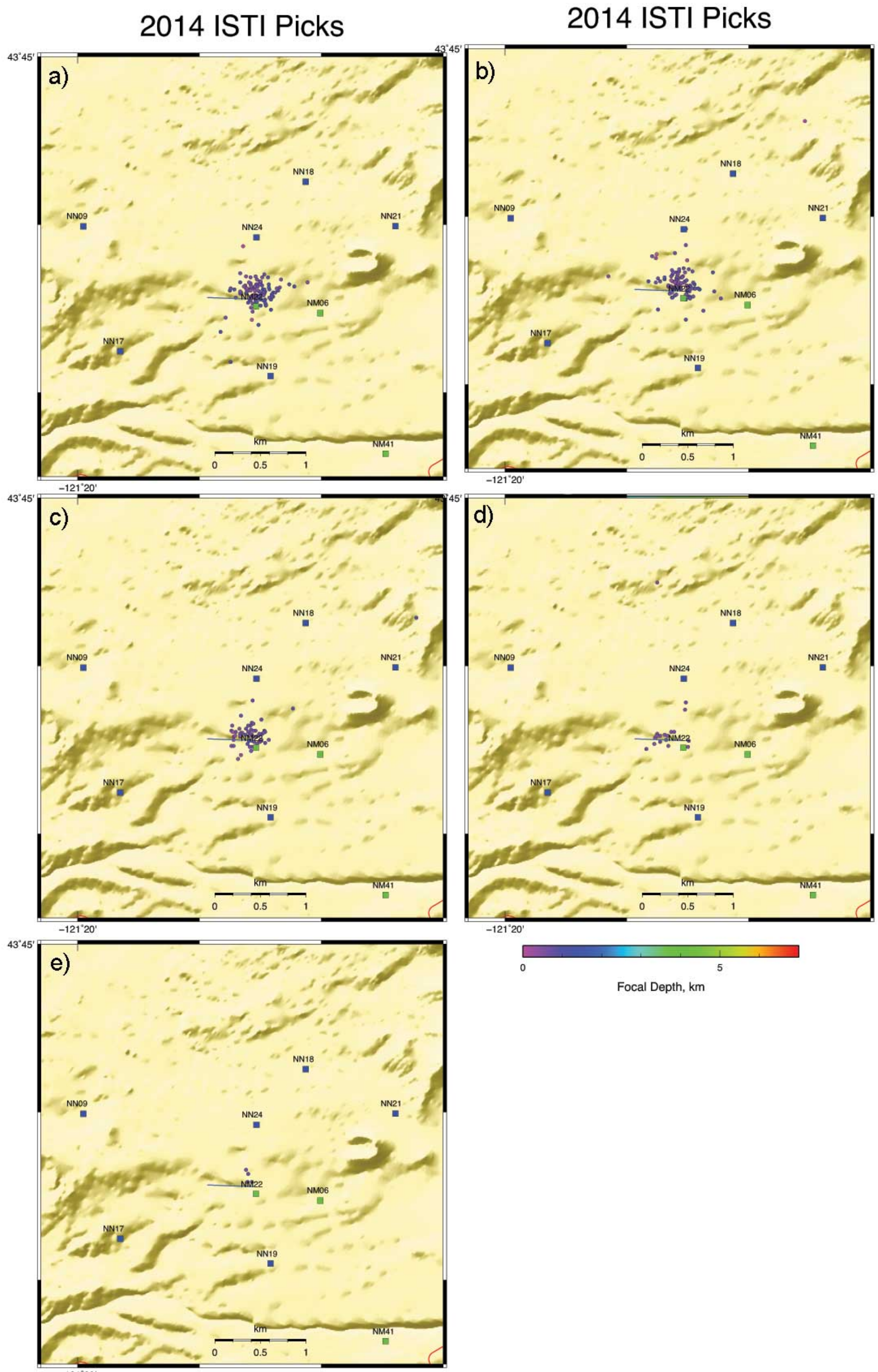

Figure 3: Hypocenters of microearthquakes within the NMSA network as a function of time. (a) 2014 Sept. 26 – Oct. 02; (b) Oct. 03 – Oct. 09; (c) Oct. 10 – Oct. 16; (d) Oct. 17 – Oct. 23; (e) Oct. 24 – Oct. 26 (shorter interval). There is no clear tendency for the events to migrate with time.

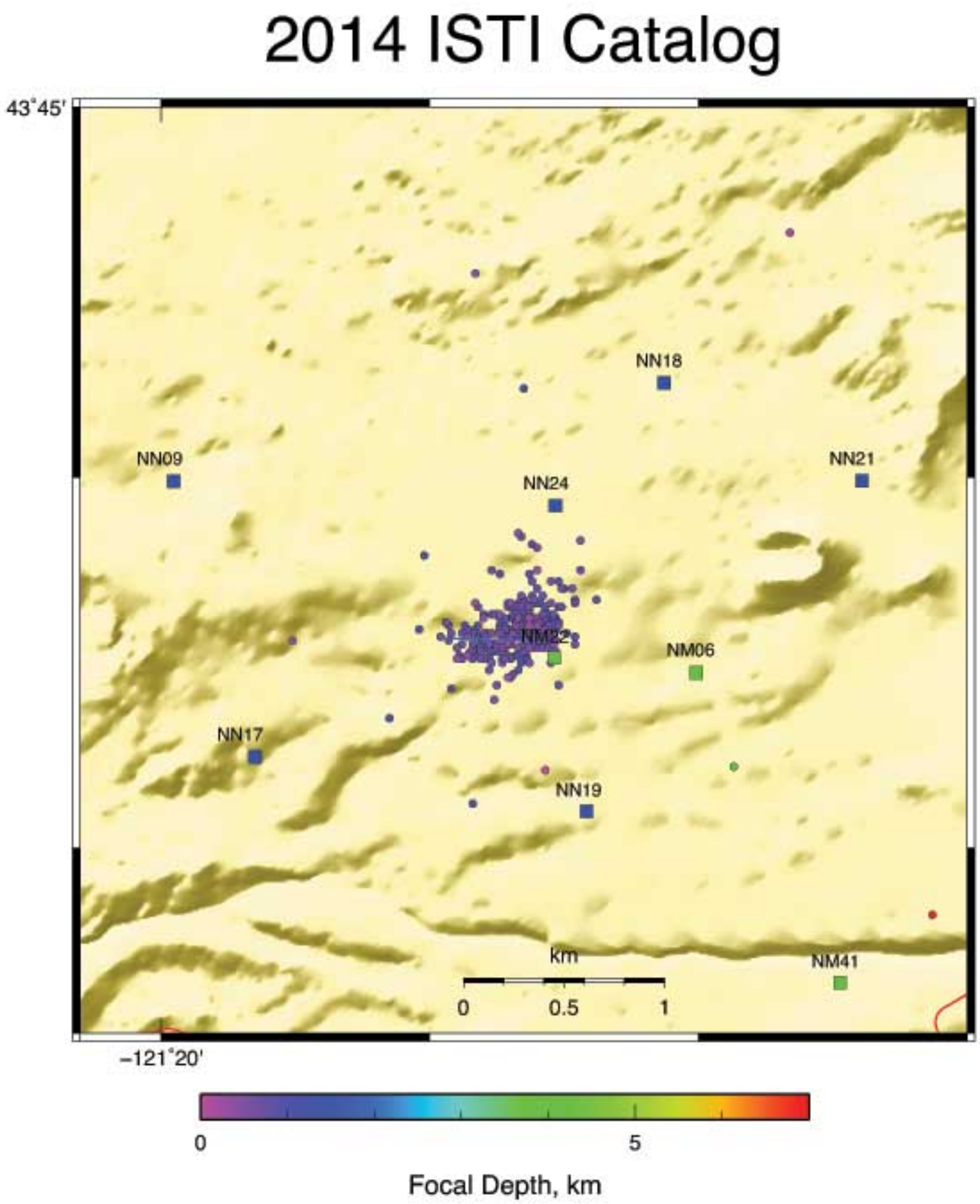

Figure 4: Hypocenters of 297 microearthquakes between Sept. 26 and Oct. 26, 2014 within the NMSA network, as given in the earthquake catalog of the ISTI Corporation. These locations are slightly but significantly west of those shown in Figure 1, which were derived from substantially the same seismic data but using a different computer program. Well NWD 55-29 is shown in blue.

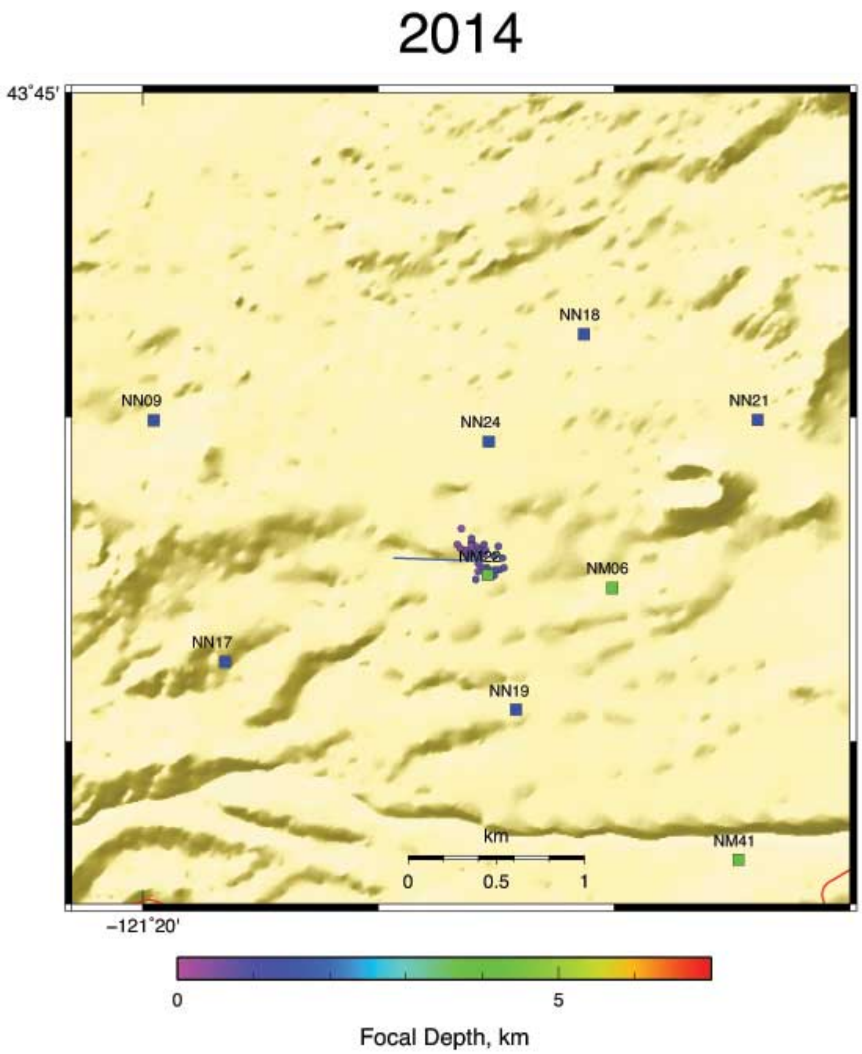

Figure 5: High quality estimated hypocenters of 34 microearthquakes that occurred between Sept. 30 and Oct. 15, 2014, and for which moment tensors were derived. These locations are computed using arrival times measured carefully in connection with the moment-tensor analysis. Well NWD 55-29 is shown in blue.

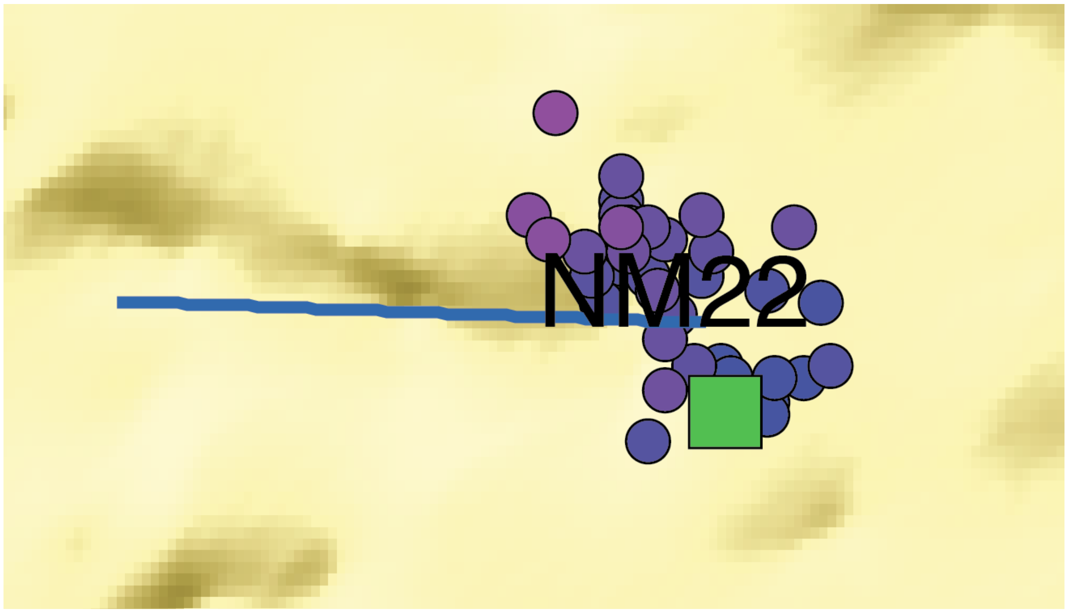

Figure 6: Expanded view of the locations of the earthquakes for which moment tensors were derived.

4.2 Relative locations

We are well advanced with the relative loction work for the earthquakes that occurred from the start of the sequence up to 19 October. We used program **hypocc**, a relative-location program based on the approach of Waldhauser and Ellsworth [2000] but written in the C programming language. This carries with it many advantages, including extreme speed. This enabled us to explored numerous run-time options to obtain the best possible result with the Newberry data.

Absolute hypocenter location methods such as the method ISTI is using, and our **qloc** locations, analyze one earthquake at a time. The results contain systematic errors caused by by errors in the crustal velocity model.

The relative location method works on a different principle, locating many earthquakes simultaneously, using as data the *differences* between the seismic-wave arrival times at common stations for pairs of earthquakes. The program divides the earthquakes into discrete "clusters" of closely grouped earthquakes, and relocates the events in each cluster relative to one another. This method greatly reduces the effect of systematic errors in the crustal model, and provides much higher resolution of the locations of nearby earthquakes *relative to other earthquakes in the same cluster.*

It is important to realize that the *absolute location of the cluster* is not improved by the relative location process. In order to fix the absolute location of the cluster, we pinnned it to a earthquake well located usign **qloc**. This was the M 1.1 earthquake of 2014 10 02 06:47:52.710, located at a latitude of 43.725296, longitude of -121.308326 and depth of 1.21 km b.s.l.

Our work proceeded as follows:

- We used the hand-measured arrival times provided by ISTI;
- We performed over 20 program runs, systematically varying three parameters in particular. These were:
    - *minclust*–the minimum number of earthquakes to define a cluster (a value of 10 was used);
    - *maxit*–the maximum allowed number of relocation iterations (optimal value identified = 25);
    - *maxsep*–the maximum separation allowed between linked pairs of earthquakes (optimal value identified = 0.15 km);
    - *minlinks*–the minimum number of "links" (i.e., measured station/phases in common between pairs of earthquakes) needed for an earthquake to be passed to the final relocated set (optimal values identified = 12 or 14);

We present two sets of results, using *minlinks* of 12 and 14.

The results using *minlinks*=12 are shown in Figure 7, Figure 8 and Figure 9. The original input dataset comprised 288 earthquakes, totalling 3411 arrival times. 129 earthquakes passed the stringent quality control parameters. Of these, 16 earthquakes failed the *maxsep* and *minclust* thresholds and were rejected as singlets. 113 earthquakes remained, comprising one cluster.

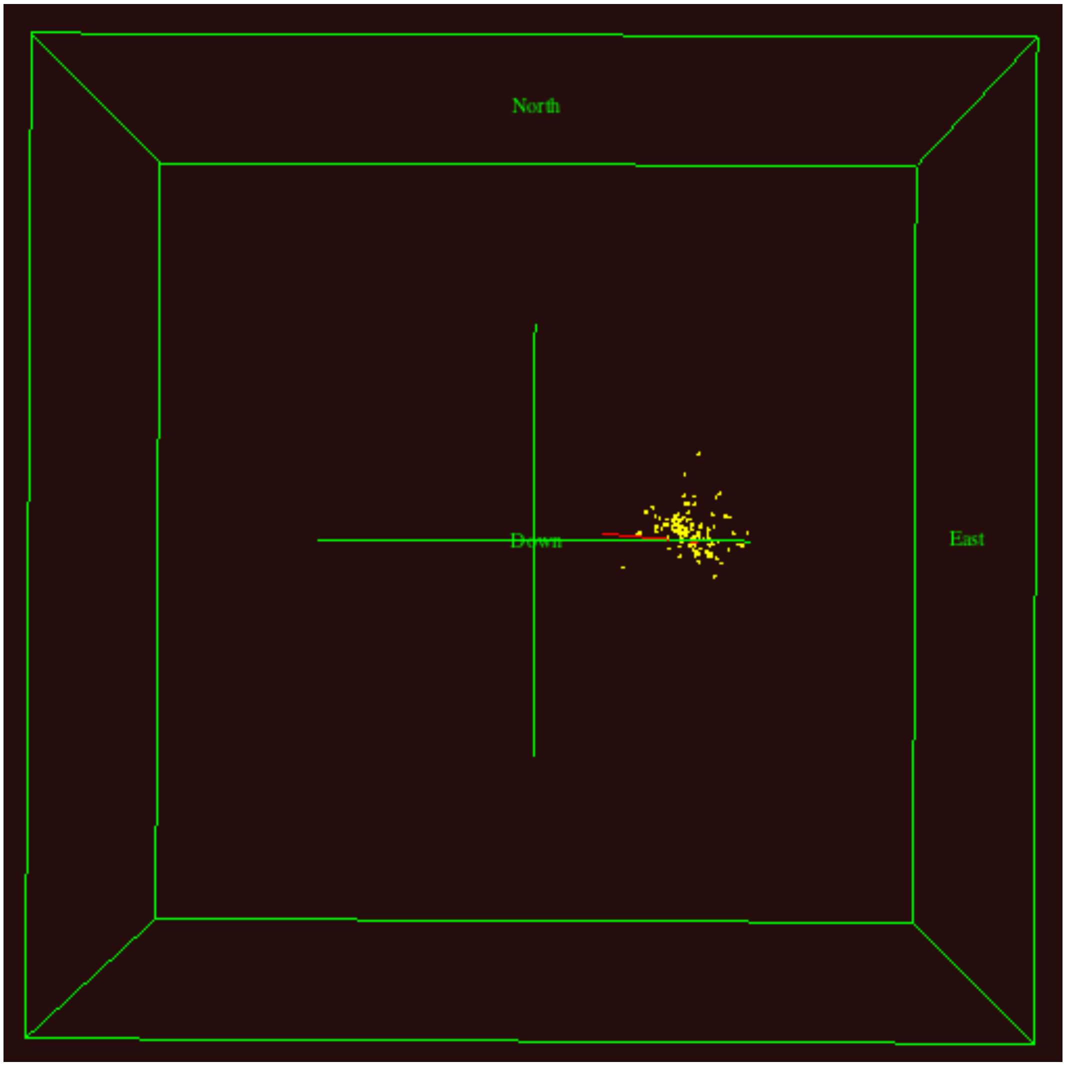

Figure 7: Map of relative locations of 113 earthquakes that occurred in the time period 26 September - 19 October, 2014. Runtime parameters used were *minclust* = 10, *maxit* = 25, *maxsep* = 0.15 km, *minlinks* = 12.

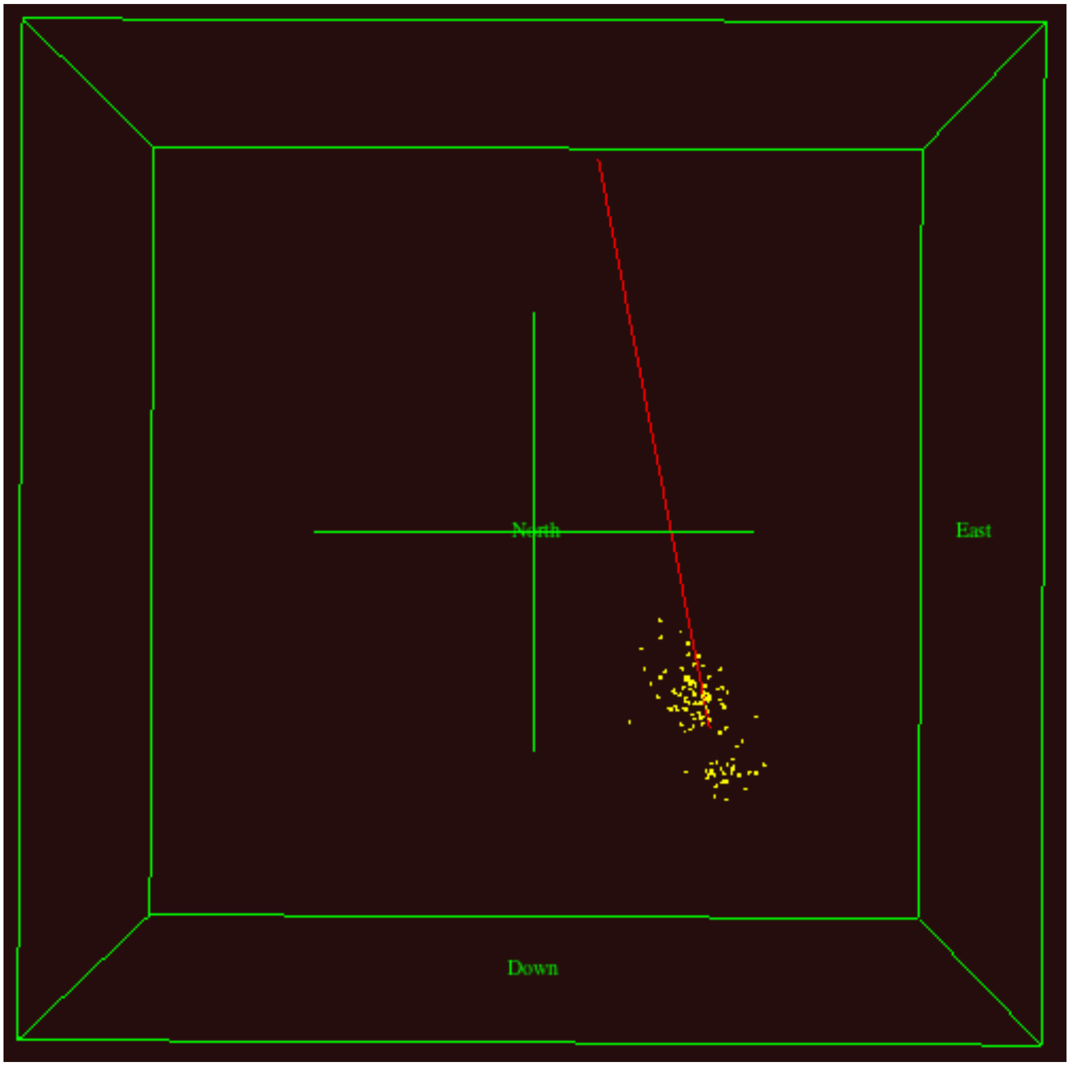

Figure 8: Same as Figure 7 except in cross section looking north.

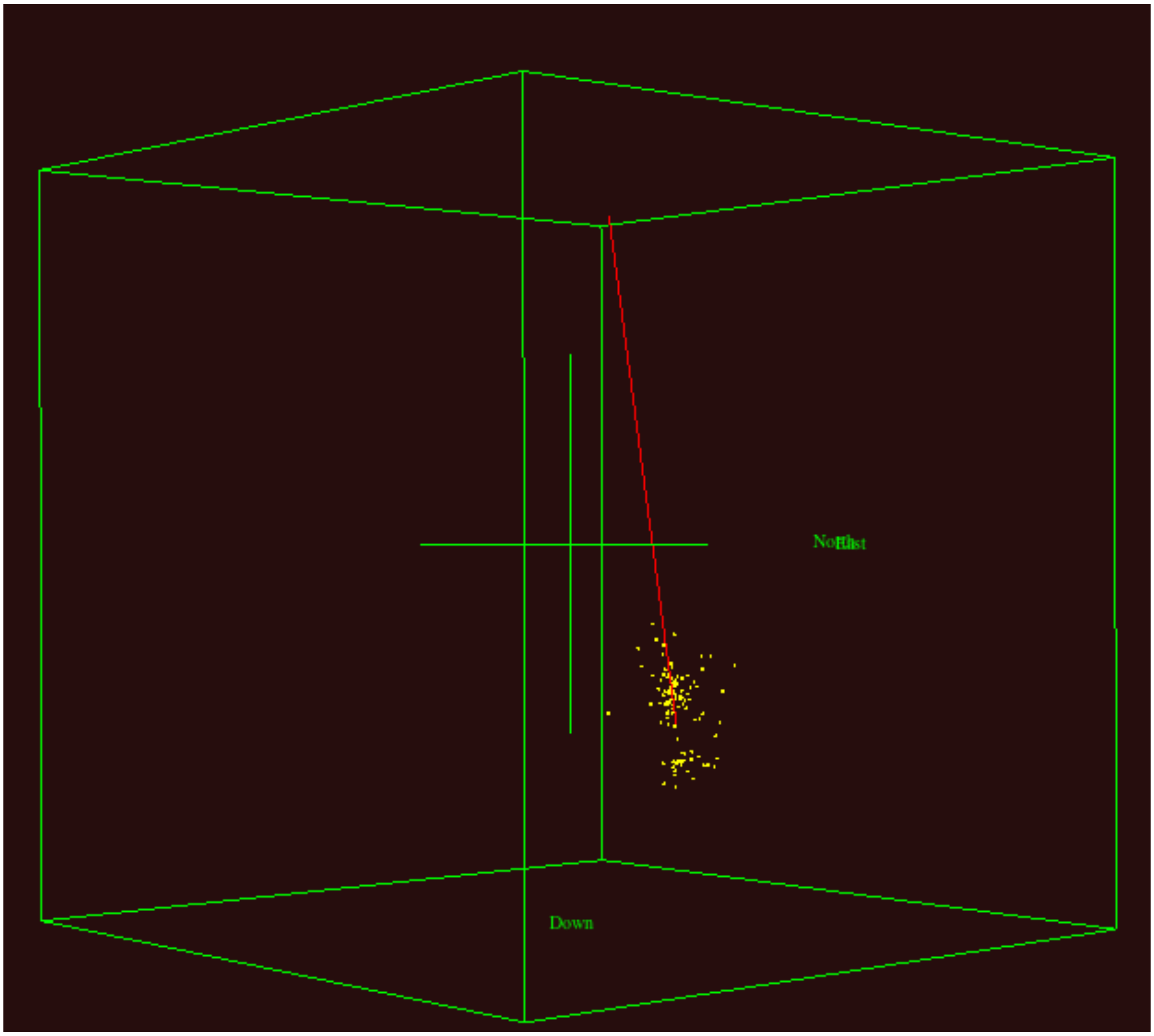

Figure 9: Same as Figure 7 except in cross section looking northwesterly, along the strike of the elongate cluster.

The results using *minlinks*=14 are shown in Figure 10, Figure 11 and Figure 12. 80 earthquakes passed the more-stringent *minlinks* setting. Of these, 14 earthquakes failed the *maxsep* and *minclust* thresholds and were rejected as singlets. 66 earthquakes remained, comprising one cluster.

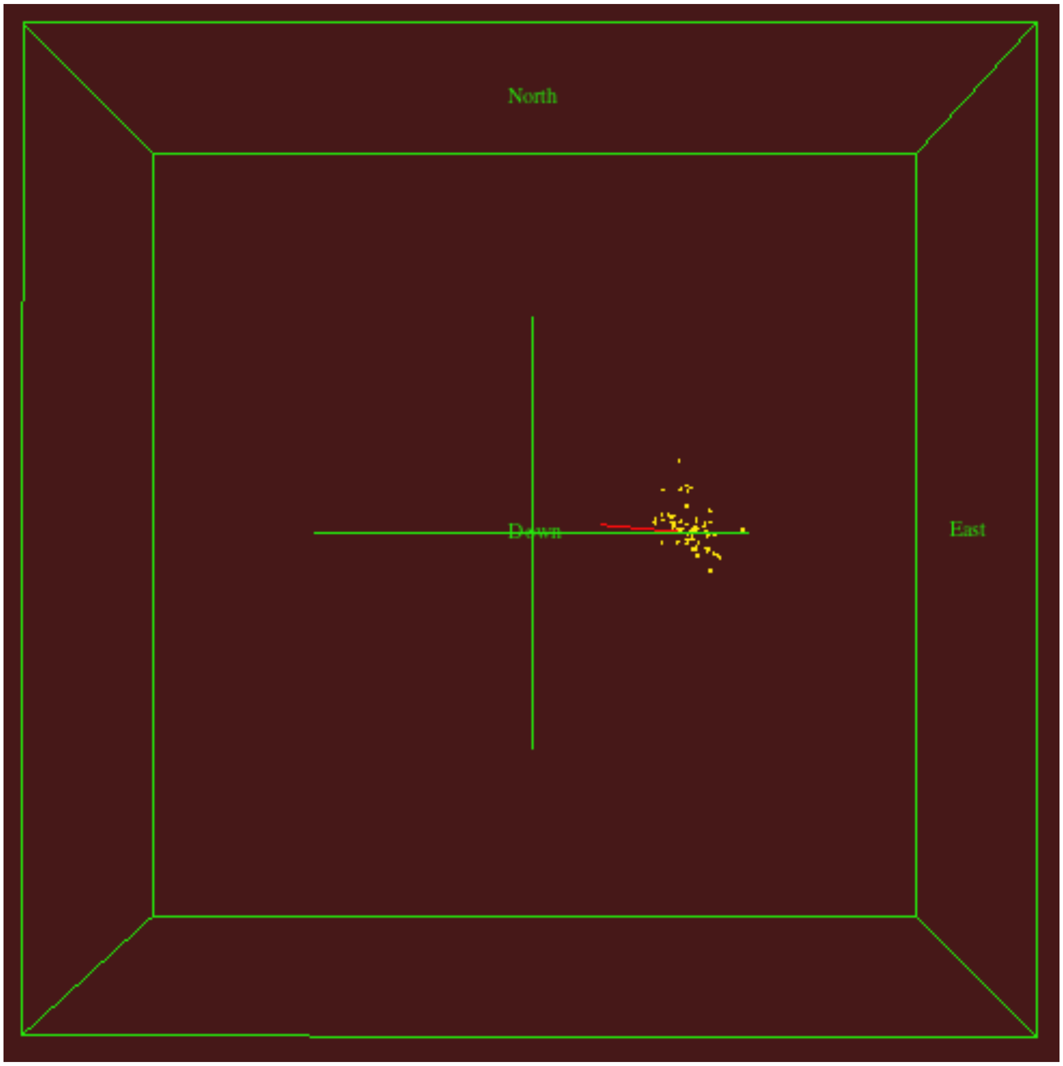

Figure 10: Map of relative locations of 66 earthquakes that occurred in the time period 26 September - 19 October, 2014. Runtime parameters used were *minclust* = 10, *maxit* = 25, *maxsep* = 0.15 km, *minlinks* = 14.

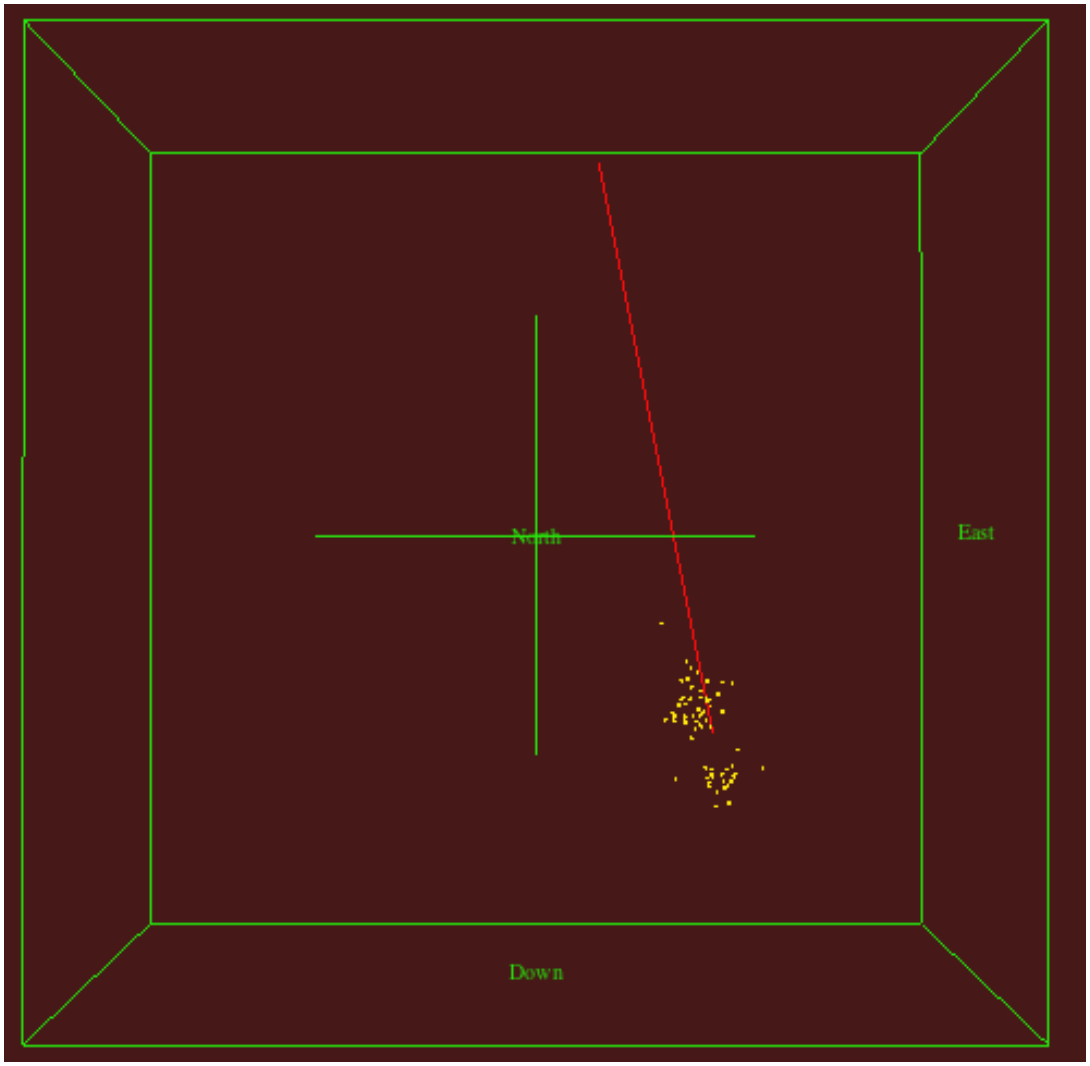

Figure 11: Same as Figure 10except in cross section looking north.

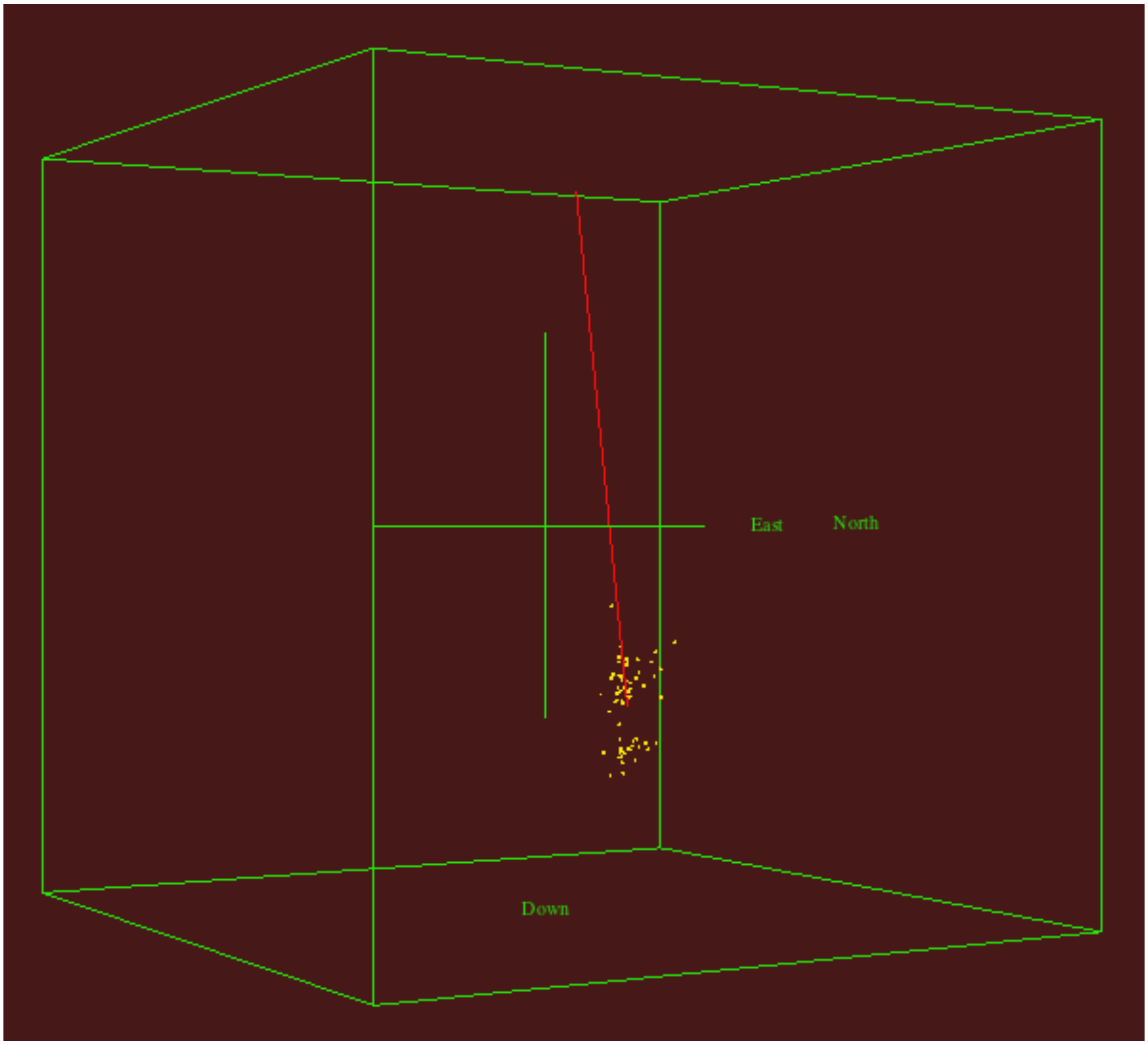

Figure 12: Same as Figure 10 except in cross section looking northwesterly, along the strike of the elongate cluster.

A brief interpretation is as follows. The epicentral region apparent in ISTI locations is quasi-circular, and the earthquake depths show a single diffuse cloud. In the **qloc** locations, more structure is visible and northwesterly orientated structure can marginally be discerned. This structure is greatly enhanced in the relative locations, which show a clear linear zone striking at N 45˚W. In depth section, the cluster clearly forms two subclusters separated by a zone ~ 200 m in depth extent that is almost devoid of earthquakes. When viewed along strike in depth section (Figure 9 and Figure 12), it can be seen that a steeply dipping structure is defined (dip ~ 87˚) that is defined most sharply on its southwesterly side.

These results suggest that the stimulation activated a northwesterly trending fault ~ 250 m in length. Two portions of the fault plane separated in depth were activated. The shallower one extends throughout approximately the lower 250 m of the borehole and the other is approximately 100 m in height, with its top about 200 m below the bottom of the well.

More work needs to be done to fine-tune and study in detail these dimensions and depths and this will comprise our work in the forthcoming week. Numerical data for these interim results have been provided to AltaRock by email attachment to Trenton Cladouhos.

5 Task 5 Moment tensor calculations

Moment tensors were derived for an additional 10 earthquakes using the same procedure as described in Weekly Report #1. The numerical results of the catalog to date are given in

Table 2. Graphical results for the additional events are shown in Appendix 1.

The source types for the entire 34-event set are shown in source-type space in Figure 13. The events form a distribution from the +Dipole to the -Dipole points, indicating a mixture of crack-opening and crack-closing events in approximately equal numbers.

Figure 14 shows a plot of the P-, T- and I-axes, approximately corresponding to the directions of σ_1, σ_3 and σ_2. The addition of more earthquakes has strengthened the distribution seen earlier whereby most T axes cluster systematically subhorizontally and to the S ± 20° or so. The orientations of the P- and I-axes are more scattered.

Table 2: Numerical moment tensor results for the 34 MEQs studied to date. N=North, E=East, D=Down.

NN	NE	EE	ND	ED	DD	Year	Mo	Day	Hr	min	Sec	Quality
1.578e-01	3.466e-02	6.671e-02	2.482e-01	6.317e-02	8.338e-02	2014	10	01	14	53	05.23	excellent
2.172e-01	-3.673e-02	-6.417e-02	2.346e-01	7.204e-02	3.184e-02	2014	10	01	19	05	16.54	excellent
8.713e-02	1.262e-01	-4.193e-02	1.814e-01	8.429e-02	8.722e-02	2014	10	04	18	51	12.00	excellent
-1.029e-01	1.325e-01	-1.185e-01	1.480e-01	5.508e-02	1.074e-01	2014	10	04	17	32	52.76	excellent
-1.165e-01	1.705e-01	-1.989e-01	1.394e-01	-2.430e-02	1.639e-02	2014	10	02	07	07	04.16	excellent
2.406e-01	-7.298e-02	-9.789e-02	1.731e-01	4.297e-02	8.349e-02	2014	10	02	11	01	42.38	excellent
-1.461e-02	9.643e-02	-3.978e-01	2.595e-02	1.691e-01	-4.693e-03	2014	10	02	06	47	52.94	excellent
6.066e-03	-2.231e-01	-9.157e-02	1.941e-01	3.367e-02	-6.184e-04	2014	10	03	06	06	22.76	excellent
-5.772e-02	-1.655e-01	-1.427e-01	1.464e-01	7.811e-02	-1.952e-02	2014	10	03	18	54	53.93	fair
2.004e-01	-1.410e-01	-1.461e-01	1.400e-01	-8.713e-03	7.412e-02	2014	10	01	12	03	16.94	good
5.304e-02	6.783e-02	-1.175e-01	1.615e-01	7.508e-02	2.206e-01	2014	10	05	04	07	20	excellent
-1.777e-01	-1.053e-01	-1.512e-01	7.111e-02	1.063e-01	1.057e-01	2014	10	01	01	03	14.49	excellent
-2.667e-01	1.320e-01	-6.399e-02	6.063e-02	1.031e-01	7.787e-02	2014	09	30	21	30	43.503	excellent

-1.871e-01	8.995e-02	-9.473e-02	-1.446e-01	-2.491e-02	1.992e-01	2014	10	05	23	22	16.499	good
1.684e-01	-3.350e-02	-9.826e-03	2.952e-01	3.542e-02	9.350e-02	2014	10	04	05	29	08.258	fair
2.449e-01	-8.111e-02	-1.972e-01	1.741e-01	1.624e-02	1.507e-02	2014	10	03	15	27	57.661	good
-2.209e-01	-8.132e-02	-2.190e-02	-1.520e-01	3.521e-02	2.201e-01	2014	10	01	16	56	11.343	good
1.477e-01	-1.175e-01	-1.492e-01	1.577e-01	-3.130e-02	9.546e-02	2014	10	01	08	08	57.998	excellent
-3.263e-02	2.220e-01	-3.373e-01	1.644e-02	7.162e-02	9.879e-03	2014	10	01	10	50	55.107	excellent
-1.038e-01	1.463e-01	-2.541e-01	1.246e-01	-1.332e-02	7.335e-02	2014	10	01	15	01	54.950	excellent
2.306e-03	-1.802e-01	-9.214e-02	2.203e-01	-4.354e-03	9.593e-02	2014	10	02	18	54	03.152	good
1.619e-01	4.200e-02	-2.041e-01	2.158e-01	-2.044e-02	7.759e-02	2014	10	02	06	39	02.998	excellent
-6.570e-02	-1.851e-01	-1.140e-01	1.691e-01	4.183e-02	2.826e-02	2014	10	02	12	39	24.317	good
1.420e-01	-1.373e-01	-1.638e-01	1.721e-01	1.076e-02	5.384e-02	2014	10	02	20	37	06.043	good
-1.365e-01	-1.837e-01	-5.911e-02	1.611e-01	-1.124e-02	9.224e-02	2014	10	05	02	06	16.967	excellent
2.866e-01	-3.707e-02	-1.787e-01	9.263e-02	1.263e-01	2.268e-02	2014	10	05	16	07	32.777	excellent
-2.286e-01	1.607e-01	-7.209e-02	-9.281e-02	8.007e-02	-3.216e-02	2014	10	05	15	55	21.007	good
-1.352e-01	-1.174e-01	-4.098e-02	1.996e-01	-5.345e-02	8.302e-02	2014	10	12	10	12	29	good
-2.211e-01	1.542e-01	4.959e-02	9.042e-02	8.191e-02	7.603e-02	2014	10	12	21	10	23.311	good
-4.882e-01	-1.017e-01	5.620e-02	5.965e-02	-1.844e-03	1.292e-01	2014	10	12	16	37	43.287	excellent
-5.873e-02	-1.252e-01	-2.804e-01	6.116e-02	1.409e-01	6.331e-03	2014	10	13	00	57	06.717	good
2.607e-02	-1.181e-01	-2.888e-01	8.025e-02	1.234e-01	4.154e-02	2014	10	13	04	12	29.126	excellent
-1.162e-01	-1.387e-01	-1.174e-01	1.514e-01	5.536e-02	7.558e-02	2014	10	13	10	22	29.084	excellent
-1.128e-01	-2.729e-02	-2.406e-01	5.661e-02	5.175e-02	3.753e-01	2014	10	14	05	46	13.914	exellent

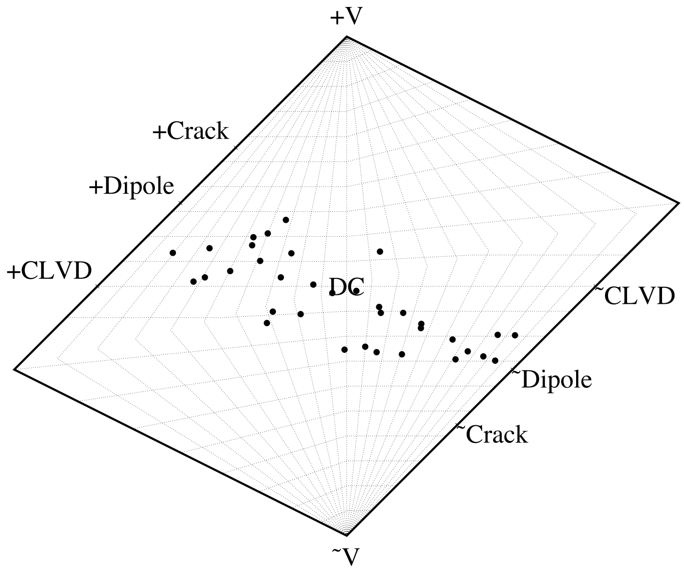

Figure 13: Source-type plot showing the earthquakes for which moment tensors have been derived to date.

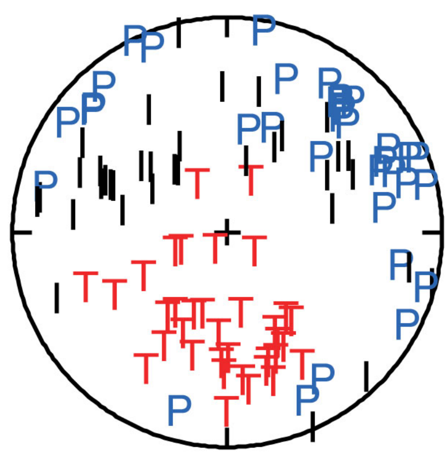

Figure 14: Plot of pressure (P ~ σ_1) and tension (T ~ σ_3) and intermediate (I ~ σ_2) axes for the 34 earthquakes for which moment tensors have been derived to date.

6 Brief summary statement

Difficulties with transferring the full data from the ISTI system to our computers have settled down. A few channels are still missing or mis-timed, but these problems are minor and not significantly impacting the quality of the results we are able to produce.

We have completed relative relocations for the earthquakes up to 19 October with good results. The earthquakes clearly define a N 45˚ W striking fault, dipping at ~ 87˚ to the NE and activated in two depth intervals. One depth interval is the lowest ~ 250 m of the borehole and the other is ~ 200 m below the bottom of the borehole. The along-strike length of the activated fault is ~ 250 m.

During the forthcoming week we will update these results with earthquakes that occurred after 19 October, and we will also relatively locate the largest earthquakes using the high-quality arrival time measurements made for moment tensor calculations.

We derived an additional 10 moment tensors, bringing the currently available set to 34. The pattern of source types observed earlier remains constant with the addition of more results. The source types range from +Dipole to -Dipole with approximately equal numbers of earthquakes showing crack-opening and crack-closure. The T-axes, which gives an indication of the direction of σ_3, cluster sub-horizontally S±20˚ or so. The P- and I-axes are more scattered.

Appendix 1: The additional nine moment tensors derived over the reporting week.

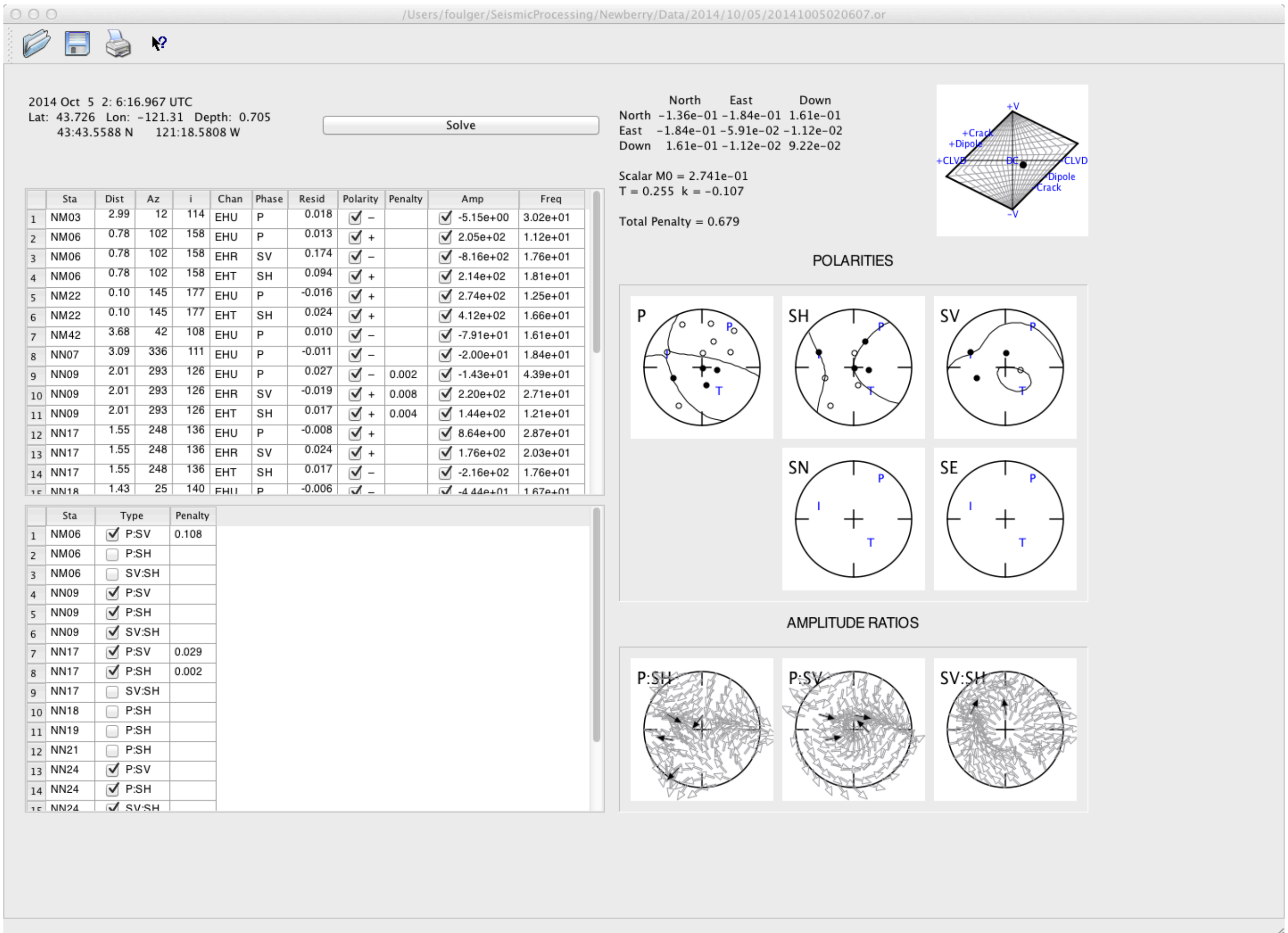

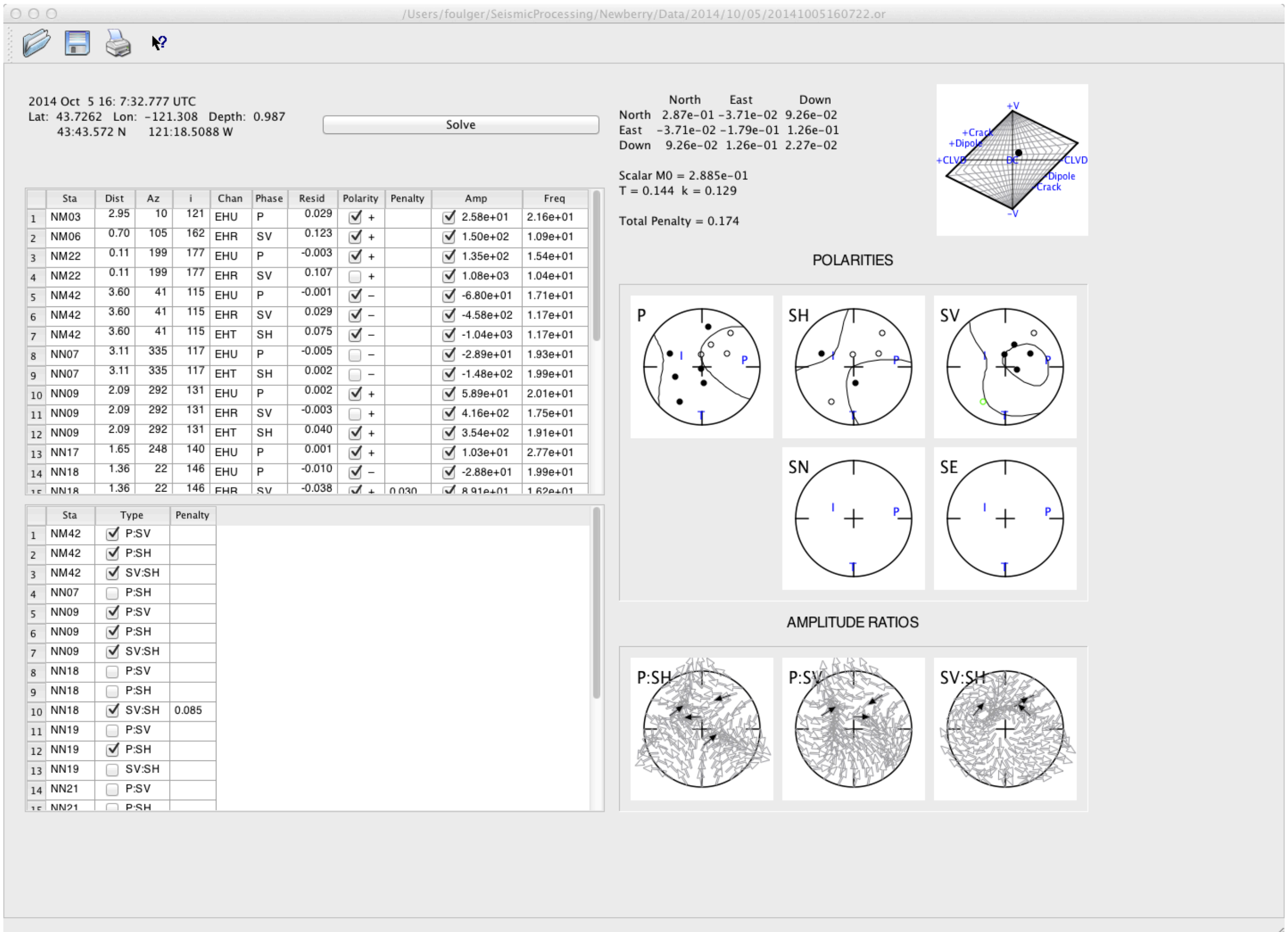
/Users/foulger/SeismicProcessing/Newberry/Data/2014/10/05/20141005160722.or
2014 Oct 5 16: 7:32.777 UTC
Lat: 43.7262 Lon: -121.308 Depth: 0.987
43:43.572 N 121:18.5088 W
Solve
North East Down
North 2.87e-01 -3.71e-02 9.26e-02
East -3.71e-02 -1.79e-01 1.26e-01
Down 9.26e-02 1.26e-01 2.27e-02
Scalar M0 = 2.885e-01
T = 0.144 k = 0.129
Total Penalty = 0.174
+V
+Crack
+Dipole
+CLVD
DC
-CLVD
-Dipole
-Crack
-V
Sta Dist Az i Chan Phase Resid Polarity Penalty Amp Freq
1 NM03 2.95 10 121 EHU P 0.029 + 2.58e+01 2.16e+01
2 NM06 0.70 105 162 EHR SV 0.123 + 1.50e+02 1.09e+01
3 NM22 0.11 199 177 EHU P -0.003 + 1.35e+02 1.54e+01
4 NM22 0.11 199 177 EHR SV 0.107 + 1.08e+03 1.04e+01
5 NM42 3.60 41 115 EHU P -0.001 – -6.80e+01 1.71e+01
6 NM42 3.60 41 115 EHR SV 0.029 – -4.58e+02 1.17e+01
7 NM42 3.60 41 115 EHT SH 0.075 – -1.04e+03 1.17e+01
8 NN07 3.11 335 117 EHU P -0.005 – -2.89e+01 1.93e+01
9 NN07 3.11 335 117 EHT SH 0.002 – -1.48e+02 1.99e+01
10 NN09 2.09 292 131 EHU P 0.002 + 5.89e+01 2.01e+01
11 NN09 2.09 292 131 EHR SV -0.003 + 4.16e+02 1.75e+01
12 NN09 2.09 292 131 EHT SH 0.040 + 3.54e+02 1.91e+01
13 NN17 1.65 248 140 EHU P 0.001 + 1.03e+01 2.77e+01
14 NN18 1.36 22 146 EHU P -0.010 – -2.88e+01 1.99e+01
Sta Type Penalty
1 NM42 P:SV
2 NM42 P:SH
3 NM42 SV:SH
4 NN07 P:SH
5 NN09 P:SV
6 NN09 P:SH
7 NN09 SV:SH
8 NN18 P:SV
9 NN18 P:SH
10 NN18 SV:SH 0.085
11 NN19 P:SV
12 NN19 P:SH
13 NN19 SV:SH
14 NN21 P:SV
POLARITIES
P
SH
SV
SN
SE
AMPLITUDE RATIOS
P:SH
P:SV
SV:SH

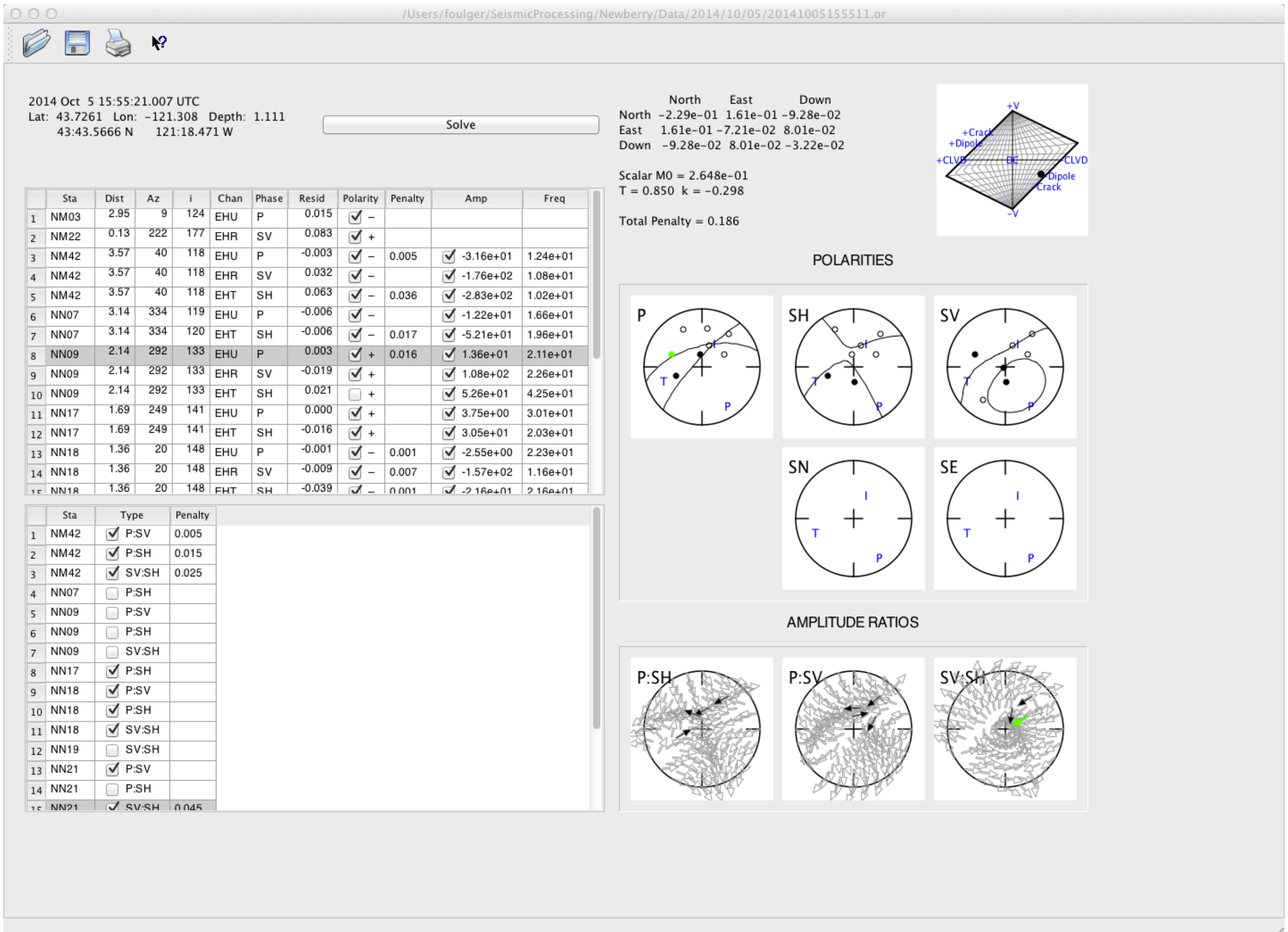

	Sta	Dist	Az	i	Chan	Phase	Resid	Polarity	Penalty	Amp	Freq
1	NM03	2.95	9	124	EHU	P	0.015	✓ –			
2	NM22	0.13	222	177	EHR	SV	0.083	✓ +			
3	NM42	3.57	40	118	EHU	P	-0.003	✓ –	0.005	✓ -3.16e+01	1.24e+01
4	NM42	3.57	40	118	EHR	SV	0.032	✓ –		✓ -1.76e+02	1.08e+01
5	NM42	3.57	40	118	EHT	SH	0.063	✓ –	0.036	✓ -2.83e+02	1.02e+01
6	NN07	3.14	334	119	EHU	P	-0.006	✓ –		✓ -1.22e+01	1.66e+01
7	NN07	3.14	334	120	EHT	SH	-0.006	✓ –	0.017	✓ -5.21e+01	1.96e+01
8	NN09	2.14	292	133	EHU	P	0.003	✓ +	0.016	✓ 1.36e+01	2.11e+01
9	NN09	2.14	292	133	EHR	SV	-0.019	✓ +		✓ 1.08e+02	2.26e+01
10	NN09	2.14	292	133	EHT	SH	0.021	☐ +		✓ 5.26e+01	4.25e+01
11	NN17	1.69	249	141	EHU	P	0.000	✓ +		✓ 3.75e+00	3.01e+01
12	NN17	1.69	249	141	EHT	SH	-0.016	✓ +		✓ 3.05e+01	2.03e+01
13	NN18	1.36	20	148	EHU	P	-0.001	✓ –	0.001	✓ -2.55e+00	2.23e+01
14	NN18	1.36	20	148	EHR	SV	-0.009	✓ –	0.007	✓ -1.57e+02	1.16e+01
15	NN18	1.36	20	148	EHT	SH	-0.039	✓ –	0.001	✓ -2.16e+01	2.16e+01

	Sta	Type	Penalty
1	NM42	✓ P:SV	0.005
2	NM42	✓ P:SH	0.015
3	NM42	✓ SV:SH	0.025
4	NN07	☐ P:SH	
5	NN09	☐ P:SV	
6	NN09	☐ P:SH	
7	NN09	☐ SV:SH	
8	NN17	✓ P:SH	
9	NN18	✓ P:SV	
10	NN18	✓ P:SH	
11	NN18	✓ SV:SH	
12	NN19	☐ SV:SH	
13	NN21	✓ P:SV	
14	NN21	☐ P:SH	
15	NN21	✓ SV:SH	0.045

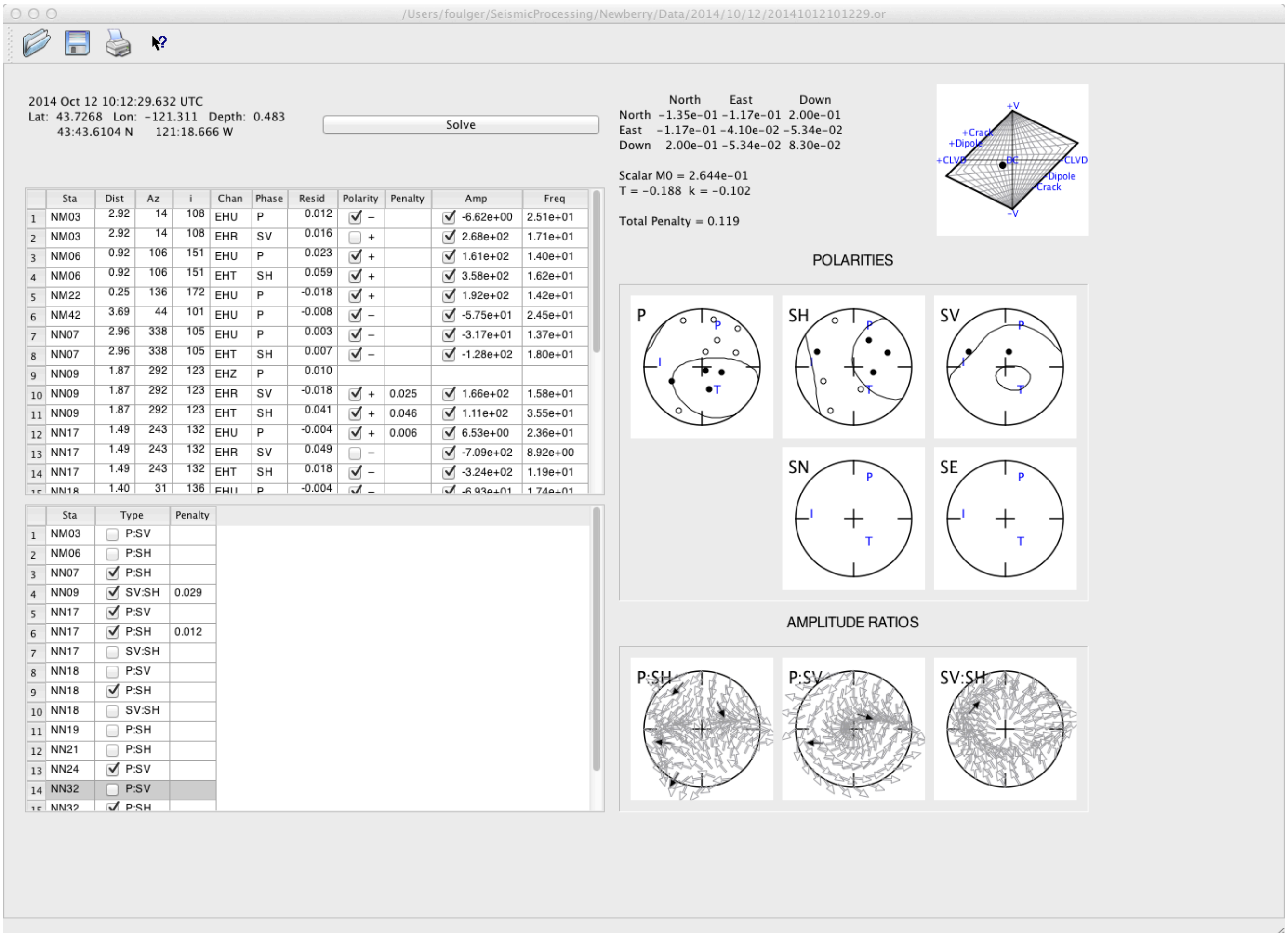

	Sta	Dist	Az	i	Chan	Phase	Resid	Polarity	Penalty	Amp	Freq
1	NM03	2.92	14	108	EHU	P	0.012	☑ –		☑ -6.62e+00	2.51e+01
2	NM03	2.92	14	108	EHR	SV	0.016	☐ +		☑ 2.68e+02	1.71e+01
3	NM06	0.92	106	151	EHU	P	0.023	☑ +		☑ 1.61e+02	1.40e+01
4	NM06	0.92	106	151	EHT	SH	0.059	☑ +		☑ 3.58e+02	1.62e+01
5	NM22	0.25	136	172	EHU	P	-0.018	☑ +		☑ 1.92e+02	1.42e+01
6	NM42	3.69	44	101	EHU	P	-0.008	☑ –		☑ -5.75e+01	2.45e+01
7	NN07	2.96	338	105	EHU	P	0.003	☑ –		☑ -3.17e+01	1.37e+01
8	NN07	2.96	338	105	EHT	SH	0.007	☑ –		☑ -1.28e+02	1.80e+01
9	NN09	1.87	292	123	EHZ	P	0.010				
10	NN09	1.87	292	123	EHR	SV	-0.018	☑ +	0.025	☑ 1.66e+02	1.58e+01
11	NN09	1.87	292	123	EHT	SH	0.041	☑ +	0.046	☑ 1.11e+02	3.55e+01
12	NN17	1.49	243	132	EHU	P	-0.004	☑ +	0.006	☑ 6.53e+00	2.36e+01
13	NN17	1.49	243	132	EHR	SV	0.049	☐ –		☑ -7.09e+02	8.92e+00
14	NN17	1.49	243	132	EHT	SH	0.018	☑ –		☑ -3.24e+02	1.19e+01
15	NN18	1.40	31	136	EHU	P	-0.004	☑ –		☑ -6.93e+01	1.74e+01

	Sta	Type	Penalty
1	NM03	☐ P:SV	
2	NM06	☐ P:SH	
3	NN07	☑ P:SH	
4	NN09	☑ SV:SH	0.029
5	NN17	☑ P:SV	
6	NN17	☑ P:SH	0.012
7	NN17	☐ SV:SH	
8	NN18	☐ P:SV	
9	NN18	☑ P:SH	
10	NN18	☐ SV:SH	
11	NN19	☐ P:SH	
12	NN21	☐ P:SH	
13	NN24	☑ P:SV	
14	NN32	☐ P:SV	
15	NN32	☑ P:SH	

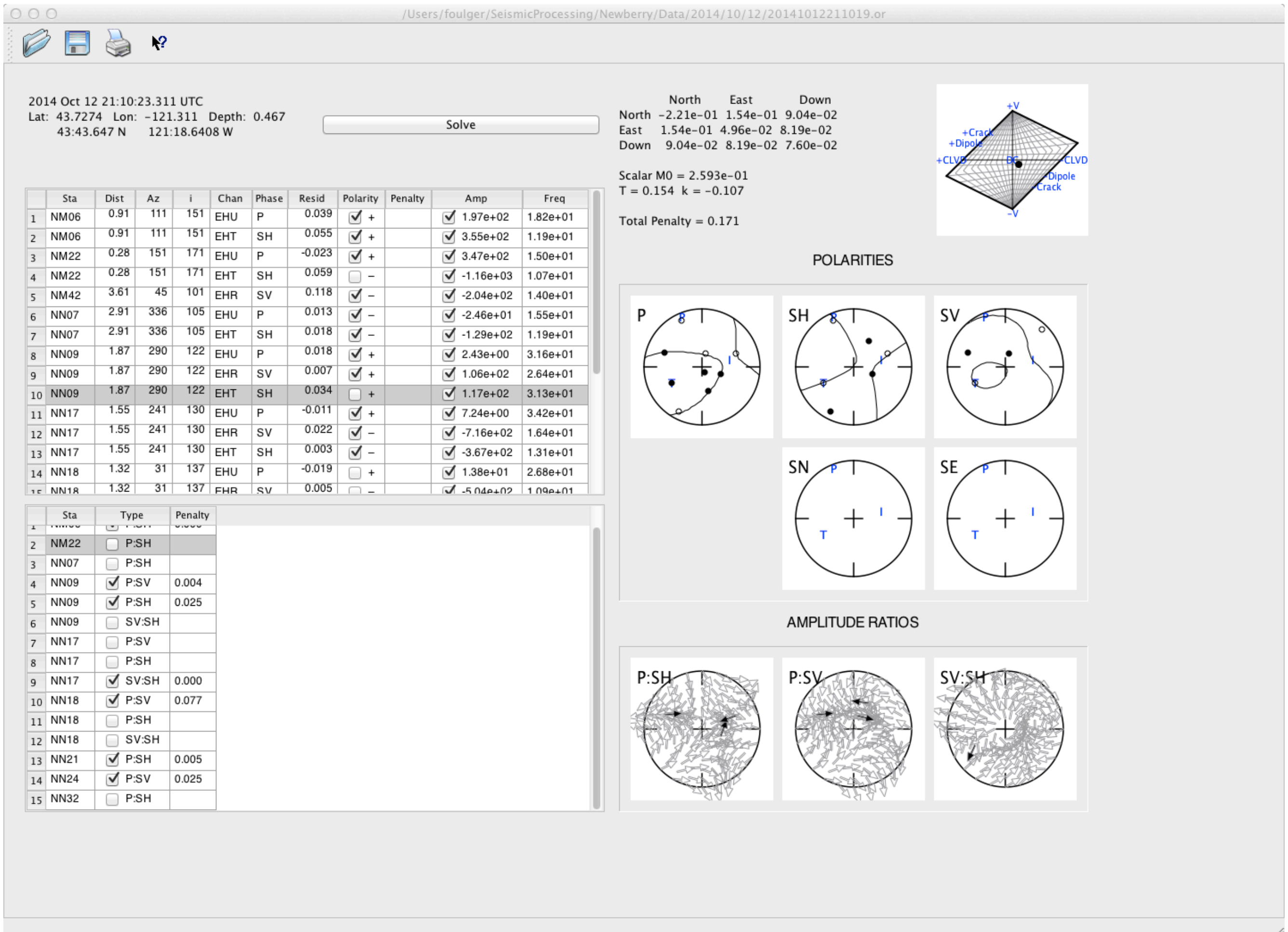

	Sta	Dist	Az	i	Chan	Phase	Resid	Polarity	Penalty	Amp	Freq
1	NM06	0.91	111	151	EHU	P	0.039	☑ +		☑ 1.97e+02	1.82e+01
2	NM06	0.91	111	151	EHT	SH	0.055	☑ +		☑ 3.55e+02	1.19e+01
3	NM22	0.28	151	171	EHU	P	-0.023	☑ +		☑ 3.47e+02	1.50e+01
4	NM22	0.28	151	171	EHT	SH	0.059	☐ –		☑ -1.16e+03	1.07e+01
5	NM42	3.61	45	101	EHR	SV	0.118	☑ –		☑ -2.04e+02	1.40e+01
6	NN07	2.91	336	105	EHU	P	0.013	☑ –		☑ -2.46e+01	1.55e+01
7	NN07	2.91	336	105	EHT	SH	0.018	☑ –		☑ -1.29e+02	1.19e+01
8	NN09	1.87	290	122	EHU	P	0.018	☑ +		☑ 2.43e+00	3.16e+01
9	NN09	1.87	290	122	EHR	SV	0.007	☑ +		☑ 1.06e+02	2.64e+01
10	NN09	1.87	290	122	EHT	SH	0.034	☐ +		☑ 1.17e+02	3.13e+01
11	NN17	1.55	241	130	EHU	P	-0.011	☑ +		☑ 7.24e+00	3.42e+01
12	NN17	1.55	241	130	EHR	SV	0.022	☑ –		☑ -7.16e+02	1.64e+01
13	NN17	1.55	241	130	EHT	SH	0.003	☑ –		☑ -3.67e+02	1.31e+01
14	NN18	1.32	31	137	EHU	P	-0.019	☐ +		☑ 1.38e+01	2.68e+01
15	NN18	1.32	31	137	EHR	SV	0.005	☐ –		☑ -5.04e+02	1.09e+01

	Sta	Type	Penalty
1	[illegible]	[illegible]	[illegible]
2	NM22	☐ P:SH	
3	NN07	☐ P:SH	
4	NN09	☑ P:SV	0.004
5	NN09	☑ P:SH	0.025
6	NN09	☐ SV:SH	
7	NN17	☐ P:SV	
8	NN17	☐ P:SH	
9	NN17	☑ SV:SH	0.000
10	NN18	☑ P:SV	0.077
11	NN18	☐ P:SH	
12	NN18	☐ SV:SH	
13	NN21	☑ P:SH	0.005
14	NN24	☑ P:SV	0.025
15	NN32	☐ P:SH	

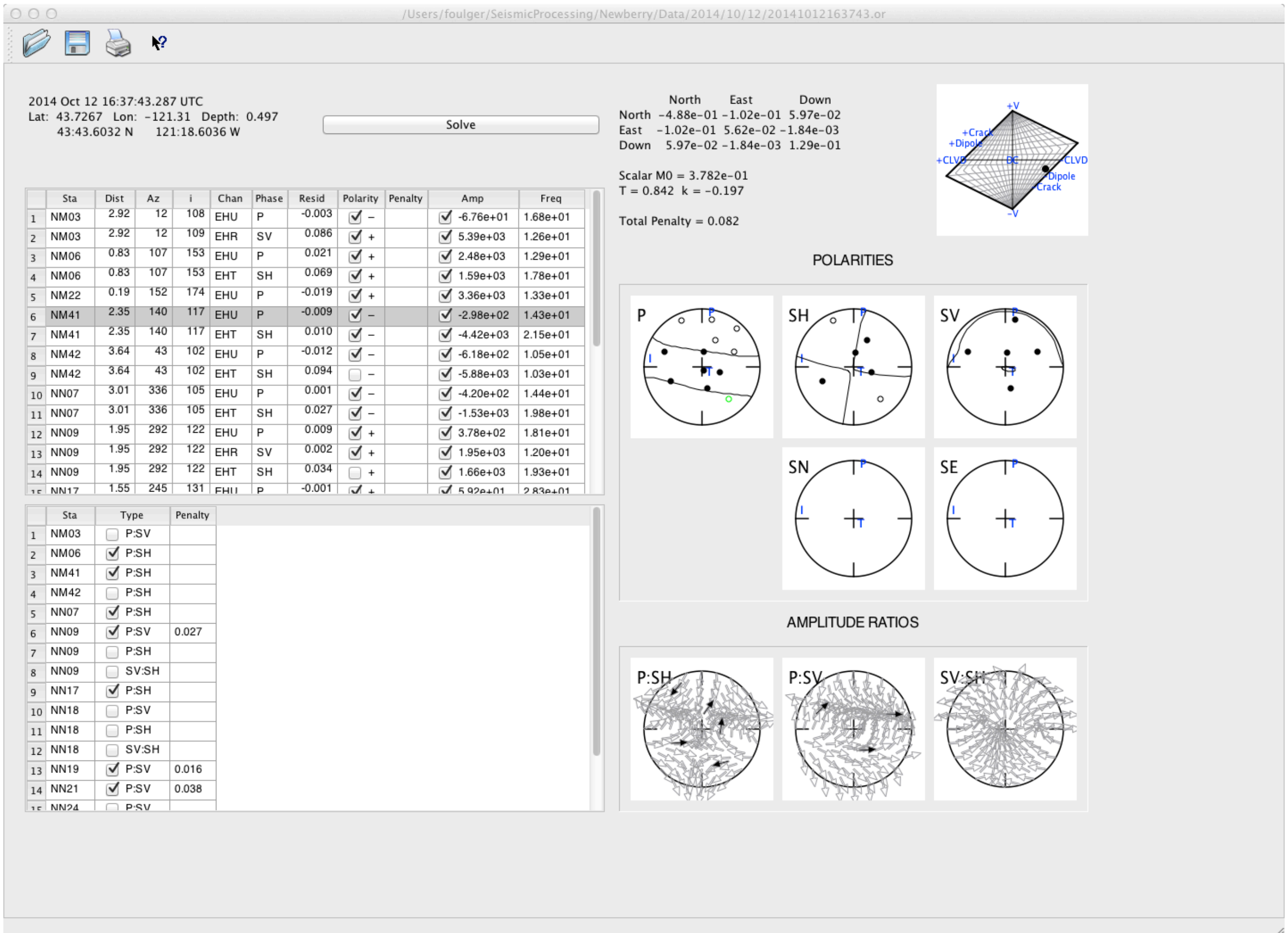

	Sta	Dist	Az	i	Chan	Phase	Resid	Polarity	Penalty	Amp	Freq
1	NM03	2.92	12	108	EHU	P	-0.003	☑ –		☑ -6.76e+01	1.68e+01
2	NM03	2.92	12	109	EHR	SV	0.086	☑ +		☑ 5.39e+03	1.26e+01
3	NM06	0.83	107	153	EHU	P	0.021	☑ +		☑ 2.48e+03	1.29e+01
4	NM06	0.83	107	153	EHT	SH	0.069	☑ +		☑ 1.59e+03	1.78e+01
5	NM22	0.19	152	174	EHU	P	-0.019	☑ +		☑ 3.36e+03	1.33e+01
6	NM41	2.35	140	117	EHU	P	-0.009	☑ –		☑ -2.98e+02	1.43e+01
7	NM41	2.35	140	117	EHT	SH	0.010	☑ –		☑ -4.42e+03	2.15e+01
8	NM42	3.64	43	102	EHU	P	-0.012	☑ –		☑ -6.18e+02	1.05e+01
9	NM42	3.64	43	102	EHT	SH	0.094	☐ –		☑ -5.88e+03	1.03e+01
10	NN07	3.01	336	105	EHU	P	0.001	☑ –		☑ -4.20e+02	1.44e+01
11	NN07	3.01	336	105	EHT	SH	0.027	☑ –		☑ -1.53e+03	1.98e+01
12	NN09	1.95	292	122	EHU	P	0.009	☑ +		☑ 3.78e+02	1.81e+01
13	NN09	1.95	292	122	EHR	SV	0.002	☑ +		☑ 1.95e+03	1.20e+01
14	NN09	1.95	292	122	EHT	SH	0.034	☐ +		☑ 1.66e+03	1.93e+01
15	NN17	1.55	245	131	EHU	P	-0.001	☑ +		☑ 5.92e+01	2.83e+01

	Sta	Type	Penalty
1	NM03	☐ P:SV	
2	NM06	☑ P:SH	
3	NM41	☑ P:SH	
4	NM42	☐ P:SH	
5	NN07	☑ P:SH	
6	NN09	☑ P:SV	0.027
7	NN09	☐ P:SH	
8	NN09	☐ SV:SH	
9	NN17	☑ P:SH	
10	NN18	☐ P:SV	
11	NN18	☐ P:SH	
12	NN18	☐ SV:SH	
13	NN19	☑ P:SV	0.016
14	NN21	☑ P:SV	0.038
15	NN24	☐ P:SV	

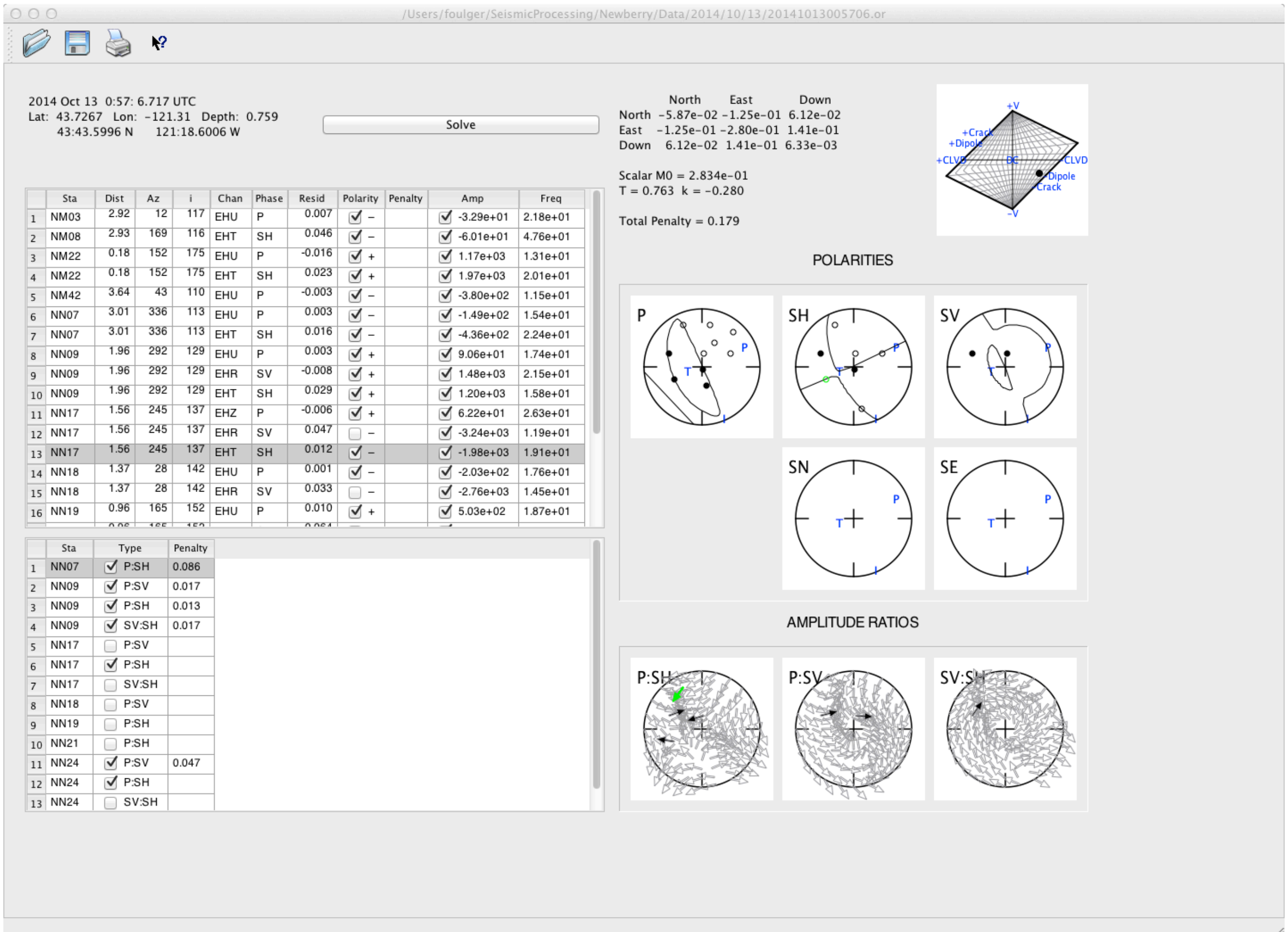

	Sta	Dist	Az	i	Chan	Phase	Resid	Polarity	Penalty	Amp	Freq
1	NM03	2.92	12	117	EHU	P	0.007	✓ –		✓ -3.29e+01	2.18e+01
2	NM08	2.93	169	116	EHT	SH	0.046	✓ –		✓ -6.01e+01	4.76e+01
3	NM22	0.18	152	175	EHU	P	-0.016	✓ +		✓ 1.17e+03	1.31e+01
4	NM22	0.18	152	175	EHT	SH	0.023	✓ +		✓ 1.97e+03	2.01e+01
5	NM42	3.64	43	110	EHU	P	-0.003	✓ –		✓ -3.80e+02	1.15e+01
6	NN07	3.01	336	113	EHU	P	0.003	✓ –		✓ -1.49e+02	1.54e+01
7	NN07	3.01	336	113	EHT	SH	0.016	✓ –		✓ -4.36e+02	2.24e+01
8	NN09	1.96	292	129	EHU	P	0.003	✓ +		✓ 9.06e+01	1.74e+01
9	NN09	1.96	292	129	EHR	SV	-0.008	✓ +		✓ 1.48e+03	2.15e+01
10	NN09	1.96	292	129	EHT	SH	0.029	✓ +		✓ 1.20e+03	1.58e+01
11	NN17	1.56	245	137	EHZ	P	-0.006	✓ +		✓ 6.22e+01	2.63e+01
12	NN17	1.56	245	137	EHR	SV	0.047	–		✓ -3.24e+03	1.19e+01
13	NN17	1.56	245	137	EHT	SH	0.012	✓ –		✓ -1.98e+03	1.91e+01
14	NN18	1.37	28	142	EHU	P	0.001	✓ –		✓ -2.03e+02	1.76e+01
15	NN18	1.37	28	142	EHR	SV	0.033	–		✓ -2.76e+03	1.45e+01
16	NN19	0.96	165	152	EHU	P	0.010	✓ +		✓ 5.03e+02	1.87e+01

	Sta	Type	Penalty
1	NN07	✓ P:SH	0.086
2	NN09	✓ P:SV	0.017
3	NN09	✓ P:SH	0.013
4	NN09	✓ SV:SH	0.017
5	NN17	P:SV	
6	NN17	✓ P:SH	
7	NN17	SV:SH	
8	NN18	P:SV	
9	NN19	P:SH	
10	NN21	P:SH	
11	NN24	✓ P:SV	0.047
12	NN24	✓ P:SH	
13	NN24	SV:SH	

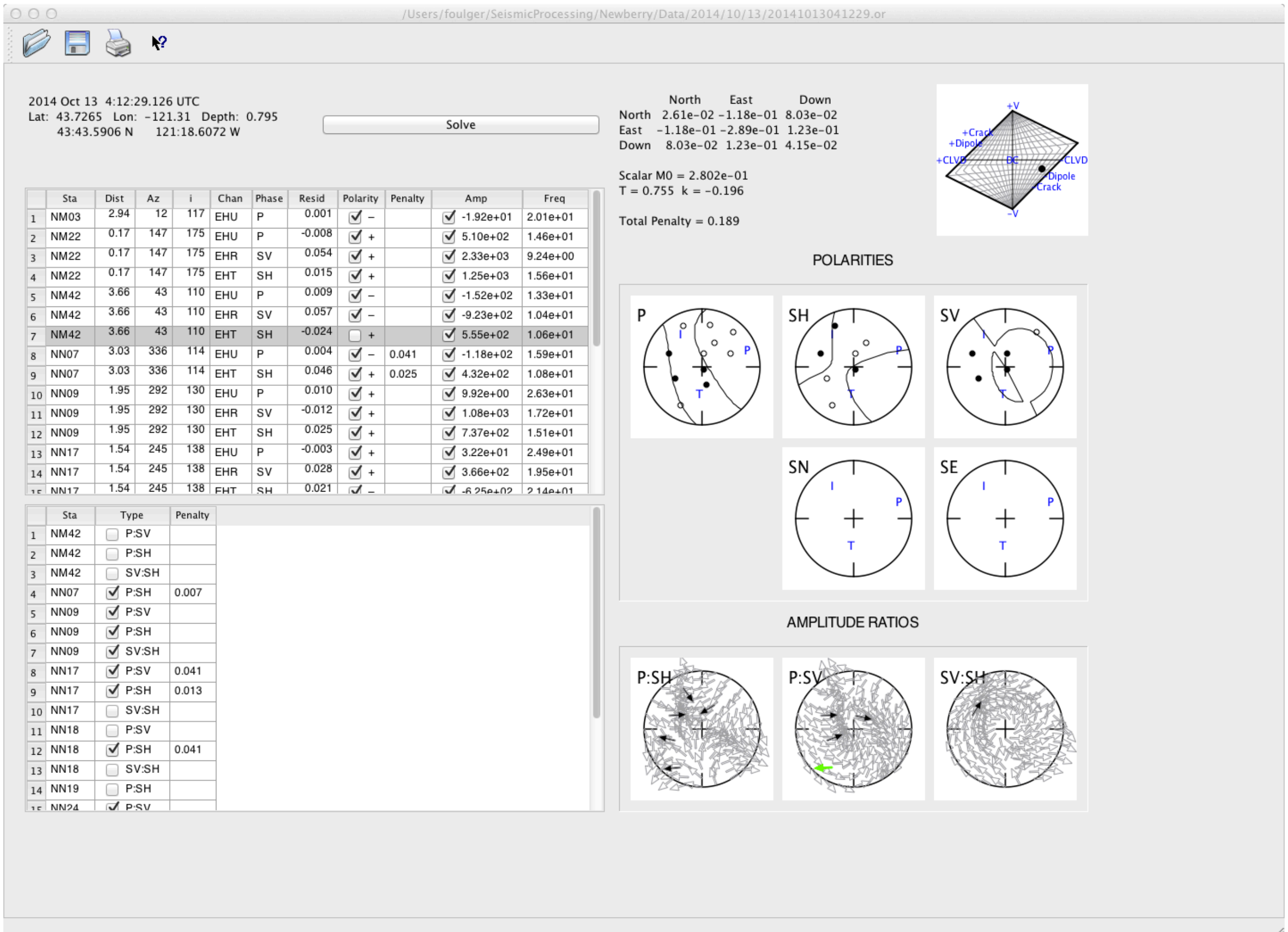
/Users/foulger/SeismicProcessing/Newberry/Data/2014/10/13/20141013041229.or
2014 Oct 13 4:12:29.126 UTC
Lat: 43.7265 Lon: -121.31 Depth: 0.795
43:43.5906 N 121:18.6072 W
Solve

	Sta	Dist	Az	i	Chan	Phase	Resid	Polarity	Penalty	Amp	Freq
1	NM03	2.94	12	117	EHU	P	0.001	✓ –		✓ -1.92e+01	2.01e+01
2	NM22	0.17	147	175	EHU	P	-0.008	✓ +		✓ 5.10e+02	1.46e+01
3	NM22	0.17	147	175	EHR	SV	0.054	✓ +		✓ 2.33e+03	9.24e+00
4	NM22	0.17	147	175	EHT	SH	0.015	✓ +		✓ 1.25e+03	1.56e+01
5	NM42	3.66	43	110	EHU	P	0.009	✓ –		✓ -1.52e+02	1.33e+01
6	NM42	3.66	43	110	EHR	SV	0.057	✓ –		✓ -9.23e+02	1.04e+01
7	NM42	3.66	43	110	EHT	SH	-0.024	☐ +		✓ 5.55e+02	1.06e+01
8	NN07	3.03	336	114	EHU	P	0.004	✓ –	0.041	✓ -1.18e+02	1.59e+01
9	NN07	3.03	336	114	EHT	SH	0.046	✓ +	0.025	✓ 4.32e+02	1.08e+01
10	NN09	1.95	292	130	EHU	P	0.010	✓ +		✓ 9.92e+00	2.63e+01
11	NN09	1.95	292	130	EHR	SV	-0.012	✓ +		✓ 1.08e+03	1.72e+01
12	NN09	1.95	292	130	EHT	SH	0.025	✓ +		✓ 7.37e+02	1.51e+01
13	NN17	1.54	245	138	EHU	P	-0.003	✓ +		✓ 3.22e+01	2.49e+01
14	NN17	1.54	245	138	EHR	SV	0.028	✓ +		✓ 3.66e+02	1.95e+01
15	NN17	1.54	245	138	EHT	SH	0.021	✓ –		✓ -6.25e+02	2.14e+01

	Sta	Type	Penalty
1	NM42	☐ P:SV	
2	NM42	☐ P:SH	
3	NM42	☐ SV:SH	
4	NN07	✓ P:SH	0.007
5	NN09	✓ P:SV	
6	NN09	✓ P:SH	
7	NN09	✓ SV:SH	
8	NN17	✓ P:SV	0.041
9	NN17	✓ P:SH	0.013
10	NN17	☐ SV:SH	
11	NN18	☐ P:SV	
12	NN18	✓ P:SH	0.041
13	NN18	☐ SV:SH	
14	NN19	☐ P:SH	
15	NN24	✓ P:SV	

North East Down
North 2.61e-02 -1.18e-01 8.03e-02
East -1.18e-01 -2.89e-01 1.23e-01
Down 8.03e-02 1.23e-01 4.15e-02
Scalar M0 = 2.802e-01
T = 0.755 k = -0.196
Total Penalty = 0.189
+V
+Crack
+Dipole
+CLVD
DC
-CLVD
-Dipole
-Crack
-V
POLARITIES
P
SH
SV
SN
SE
AMPLITUDE RATIOS
P:SH
P:SV
SV:SH

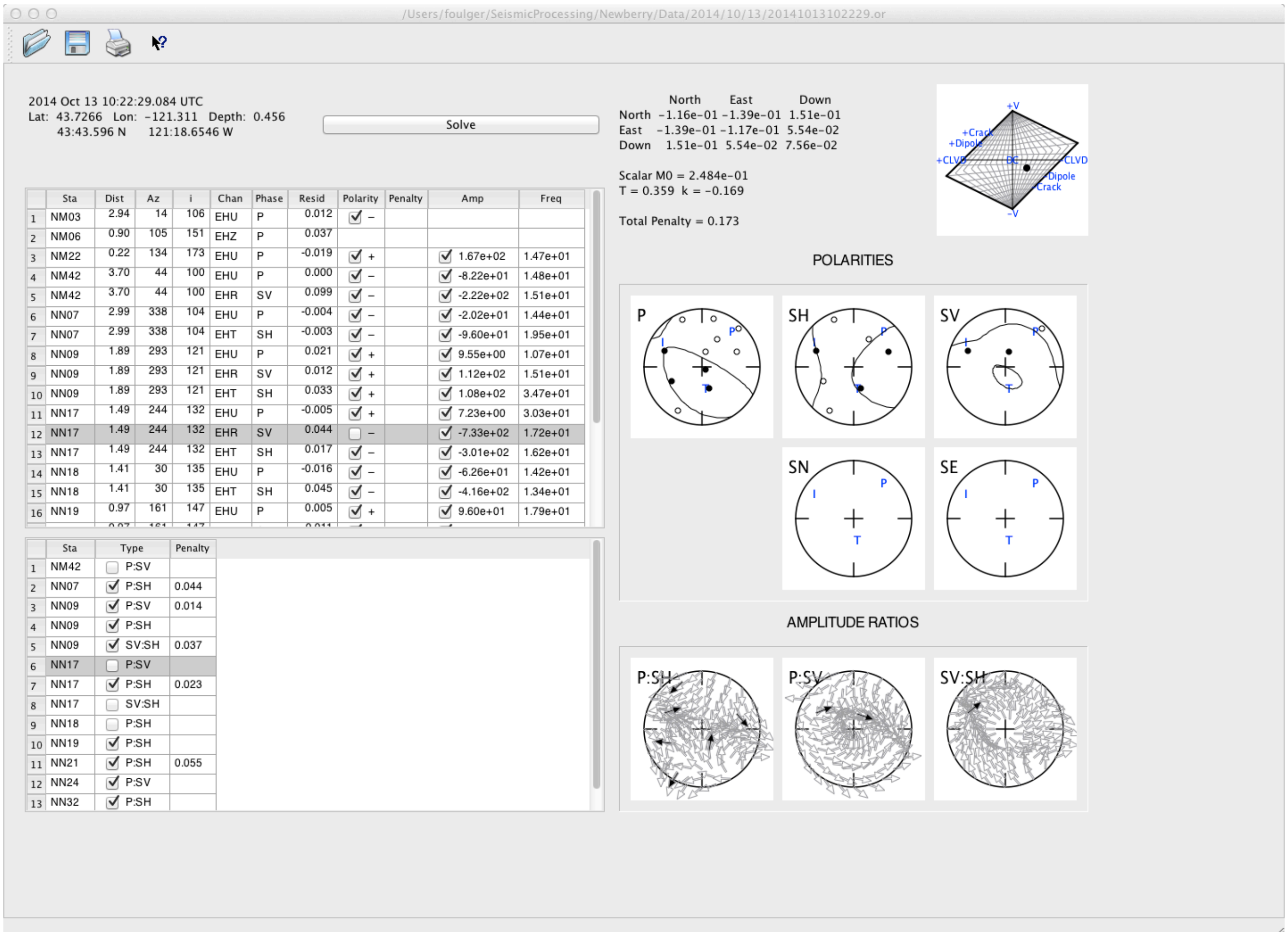

	Sta	Dist	Az	i	Chan	Phase	Resid	Polarity	Penalty	Amp	Freq
1	NM03	2.94	14	106	EHU	P	0.012	✓ −			
2	NM06	0.90	105	151	EHZ	P	0.037				
3	NM22	0.22	134	173	EHU	P	-0.019	✓ +		✓ 1.67e+02	1.47e+01
4	NM42	3.70	44	100	EHU	P	0.000	✓ −		✓ -8.22e+01	1.48e+01
5	NM42	3.70	44	100	EHR	SV	0.099	✓ −		✓ -2.22e+02	1.51e+01
6	NN07	2.99	338	104	EHU	P	-0.004	✓ −		✓ -2.02e+01	1.44e+01
7	NN07	2.99	338	104	EHT	SH	-0.003	✓ −		✓ -9.60e+01	1.95e+01
8	NN09	1.89	293	121	EHU	P	0.021	✓ +		✓ 9.55e+00	1.07e+01
9	NN09	1.89	293	121	EHR	SV	0.012	✓ +		✓ 1.12e+02	1.51e+01
10	NN09	1.89	293	121	EHT	SH	0.033	✓ +		✓ 1.08e+02	3.47e+01
11	NN17	1.49	244	132	EHU	P	-0.005	✓ +		✓ 7.23e+00	3.03e+01
12	NN17	1.49	244	132	EHR	SV	0.044	☐ −		✓ -7.33e+02	1.72e+01
13	NN17	1.49	244	132	EHT	SH	0.017	✓ −		✓ -3.01e+02	1.62e+01
14	NN18	1.41	30	135	EHU	P	-0.016	✓ −		✓ -6.26e+01	1.42e+01
15	NN18	1.41	30	135	EHT	SH	0.045	✓ −		✓ -4.16e+02	1.34e+01
16	NN19	0.97	161	147	EHU	P	0.005	✓ +		✓ 9.60e+01	1.79e+01

	Sta	Type	Penalty
1	NM42	☐ P:SV	
2	NN07	✓ P:SH	0.044
3	NN09	✓ P:SV	0.014
4	NN09	✓ P:SH	
5	NN09	✓ SV:SH	0.037
6	NN17	☐ P:SV	
7	NN17	✓ P:SH	0.023
8	NN17	☐ SV:SH	
9	NN18	☐ P:SH	
10	NN19	✓ P:SH	
11	NN21	✓ P:SH	0.055
12	NN24	✓ P:SV	
13	NN32	✓ P:SH	

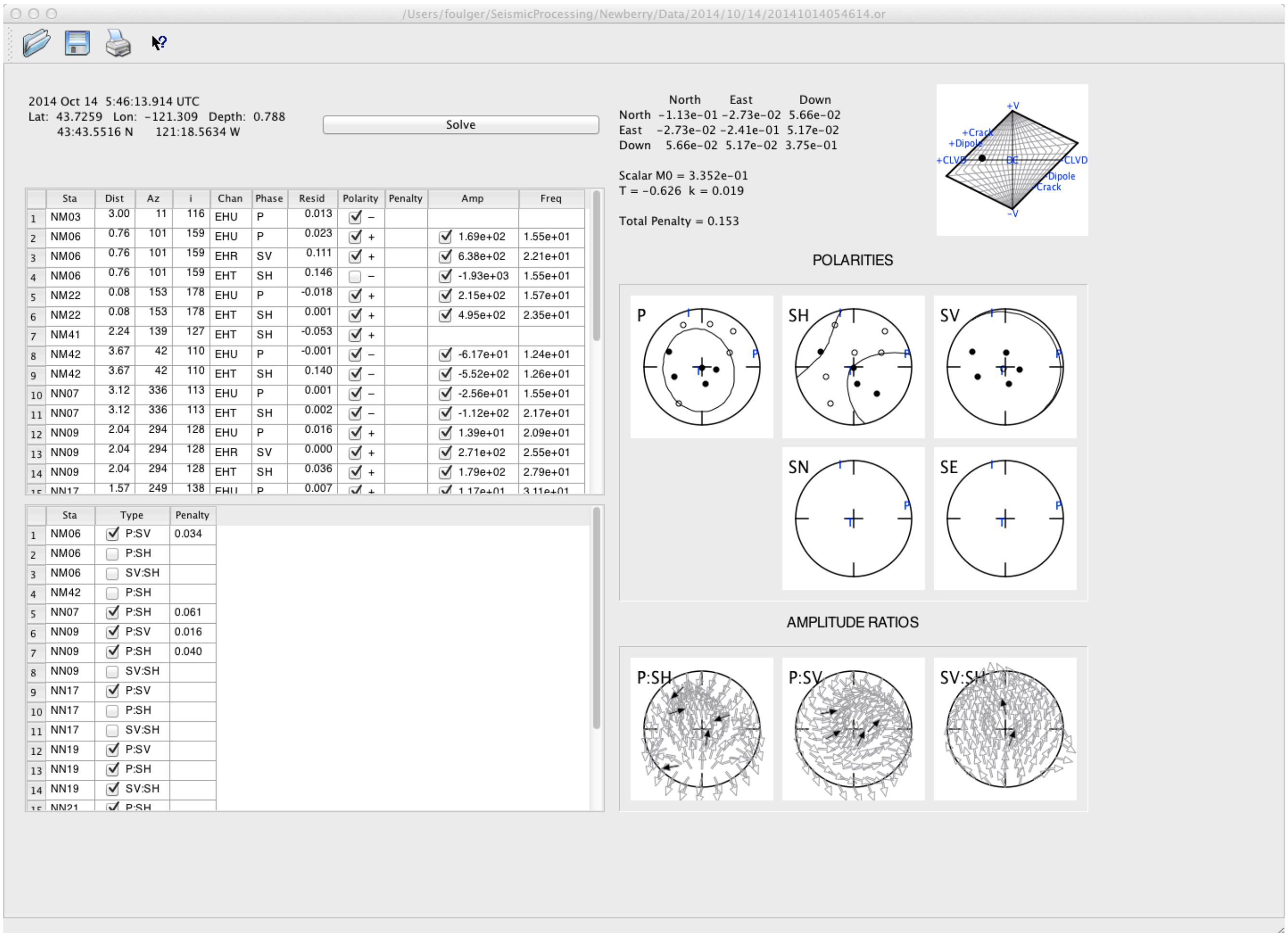
/Users/foulger/SeismicProcessing/Newberry/Data/2014/10/14/20141014054614.or
2014 Oct 14 5:46:13.914 UTC
Lat: 43.7259 Lon: -121.309 Depth: 0.788
43:43.5516 N 121:18.5634 W
Solve
North East Down
North -1.13e-01 -2.73e-02 5.66e-02
East -2.73e-02 -2.41e-01 5.17e-02
Down 5.66e-02 5.17e-02 3.75e-01
Scalar M0 = 3.352e-01
T = -0.626 k = 0.019
Total Penalty = 0.153
+V
+Crack
+Dipole
+CLVD
DC
-CLVD
-Dipole
-Crack
-V
Sta Dist Az i Chan Phase Resid Polarity Penalty Amp Freq
1 NM03 3.00 11 116 EHU P 0.013 –
2 NM06 0.76 101 159 EHU P 0.023 + 1.69e+02 1.55e+01
3 NM06 0.76 101 159 EHR SV 0.111 + 6.38e+02 2.21e+01
4 NM06 0.76 101 159 EHT SH 0.146 – -1.93e+03 1.55e+01
5 NM22 0.08 153 178 EHU P -0.018 + 2.15e+02 1.57e+01
6 NM22 0.08 153 178 EHT SH 0.001 + 4.95e+02 2.35e+01
7 NM41 2.24 139 127 EHT SH -0.053 +
8 NM42 3.67 42 110 EHU P -0.001 – -6.17e+01 1.24e+01
9 NM42 3.67 42 110 EHT SH 0.140 – -5.52e+02 1.26e+01
10 NN07 3.12 336 113 EHU P 0.001 – -2.56e+01 1.55e+01
11 NN07 3.12 336 113 EHT SH 0.002 – -1.12e+02 2.17e+01
12 NN09 2.04 294 128 EHU P 0.016 + 1.39e+01 2.09e+01
13 NN09 2.04 294 128 EHR SV 0.000 + 2.71e+02 2.55e+01
14 NN09 2.04 294 128 EHT SH 0.036 + 1.79e+02 2.79e+01
Sta Type Penalty
1 NM06 P:SV 0.034
2 NM06 P:SH
3 NM06 SV:SH
4 NM42 P:SH
5 NN07 P:SH 0.061
6 NN09 P:SV 0.016
7 NN09 P:SH 0.040
8 NN09 SV:SH
9 NN17 P:SV
10 NN17 P:SH
11 NN17 SV:SH
12 NN19 P:SV
13 NN19 P:SH
14 NN19 SV:SH
POLARITIES
P
SH
SV
SN
SE
AMPLITUDE RATIOS
P:SH
P:SV
SV:SH